NATIONAL ADVISORY COMMITTEE FOR AERONAUTICS

WARTIME REPORT

ORIGINALLY ISSUED
November 1945 as
Advance Confidential Report L5I04

AN INFRARED CLOUD INDICATOR

I - ANALYSIS OF INFRARED-RADIATION EXCHANGE WITH TABLES AND CHART FOR CALIBRATION OF THE CLOUD INDICATOR

By Calvin N. Warfield and Robert L. Kenimer

Langley Memorial Aeronautical Laboratory
Langley Field, Va.

NACA

WASHINGTON

NACA ACR No. L5I04 [redacted]

NATIONAL ADVISORY COMMITTEE FOR AERONAUTICS

ADVANCE CONFIDENTIAL REPORT

AN INFRARED CLOUD INDICATOR

I - ANALYSIS OF INFRARED-RADIATION EXCHANGE WITH TABLES AND CHART FOR CALIBRATION OF THE CLOUD INDICATOR

By Calvin N. Warfield and Robert L. Kenimer

SUMMARY

An experimental model of a flight instrument that utilizes infrared radiations for detecting and indicating the location of clouds at night is briefly described. In order to determine the important parameters that contribute to the net exchange of radiation between the receiver of the cloud indicator and a cloud, a preliminary investigation is made of data in the scientific literature. The important parameters are then used in an analysis of the net exchange of radiation between the receiver of the cloud indicator and a cloud. As a result of the analysis, several tables and a chart have been devised, which make it practical to determine the magnitude of the net exchange of radiation for any particular atmosphere of known composition and distribution of temperature. The analysis and the resulting tables and chart take into consideration both water vapor and carbon dioxide and also the effect of the spectral absorption and emission of the optical system of the cloud indicator.

The tables and the chart that resulted from the analysis were devised to provide a basis for extrapolating the results of ground observations to the range anticipated during flight use.

INTRODUCTION

As a result of a number of airline accidents that are attributable in part to inadequate weather forecasts or to the inability of the pilot to estimate correctly the turbulence of the atmosphere, an experimental model of a flight instrument designed to assist pilots in avoiding highly

turbulent regions during night flights has been developed at the Langley Laboratory. The perfection of such an instrument should increase the safety of flight and may ultimately make possible a reduction of the design gust load factor.

Although clouds are frequently associated with regions of high atmospheric turbulence, some clouds are almost wholly devoid of turbulence. The original objective of the present project therefore was to devise an instrument that would indicate the degree of turbulence of clouds at a distance. A preliminary investigation failed to reveal any practical means of indicating the degree of turbulence of clouds at a distance. The immediate practical objective was therefore limited to the development of a device utilizing infrared radiation that locates clouds at night and thereby enables the pilot to avoid them. Such an instrument should also be useful in weather-reconnaissance flights at night to assist in the observation of cloud formations. An experimental model of such a device has been constructed and is referred to herein as the "cloud indicator."

The indicating meter of the cloud indicator should be calibrated to enable the pilot to read directly the distance to the cloud on which the instrument is sighted. A direct calibration of the cloud indicator could be obtained by making numerous flights with the instrument under various atmospheric conditions. A number of flights were made which conclusively demonstrated that the cloud indicator could detect the presence of clouds at night when they could not be seen with the unaided eye. Plans for a direct calibration of the cloud indicator by a series of measurements in flight, however, had to be abandoned because of the difficulty and expense of simultaneously measuring the net exchange of radiation and the height and distance of the cloud sighted on relative to the airplane on which the instrument is mounted. It has therefore been necessary to rely upon measurements made with the instrument mounted on roof tops or on the ground at Langley Field, Va. Because these ground observations cover only a part of the range of atmospheric conditions and distances to be encountered in flight observations, extrapolation of the results of the ground observations is necessary.

[redacted]

Because of the widely varying conditions under which the ground observations were made, extrapolation into the range expected in flight is possible only by means of computations based on an analysis of the net exchange of radiation. The present project was therefore extended to include an analysis of the net exchange of radiation involved in the calibration of the indicating meter of the cloud indicator. This analysis is used in computing the net radiation exchange for the atmospheric conditions that existed during the ground observations, and these values are correlated with the readings of the indicating meter. The analysis is then used in designing a scale for the indicating meter to cover all ranges of atmospheric conditions anticipated for flight use.

The present report includes a brief statement of the fundamental principles involved and a brief description of the cloud indicator. Results are given of a preliminary investigation that was necessary before the analysis was started to determine the important parameters which contribute to the net exchange of radiation. This investigation is based upon data found in existing scientific literature.

As an aid in applying the analysis to the calibration of the cloud indicator, a number of tables and a radiation chart have been constructed and are included in the present report. Examples of the use of the tables and chart are also given herein.

FUNDAMENTAL PRINCIPLES AND DESCRIPTION OF CLOUD INDICATOR

The thermal emission of infrared radiation is the fundamental physical property upon which the cloud indicator is based. Every substance emits some of this infrared radiation with an intensity and a spectral distribution that are determined by its nature and temperature. For substances within the range of atmospheric temperatures, all the thermal radiation of any significant intensity lies in the part of the invisible spectrum that is beyond the range of infrared photography and of infrared photoelectric cells. The sensitive element of the cloud indicator must therefore respond to these relatively long infrared radiations. For the present experimental model of the cloud indicator, a sensitive

quick-response five-junction thermopile equipped with a blackened receiver that responds to the entire infrared spectrum has been chosen as the sensitive element. The so-called cold junctions of the thermopile are kept at the temperature of the thermopile housing. The other junctions are exposed to radiation that originates outside the housing.

Within the region of the spectrum in which the thermal emissions at atmospheric temperatures are found, the liquid-water content of all except thin transparent clouds emits radiation with an intensity about as great as that of any other substance. The clear atmosphere, however, emits much less radiation in this same spectral region. An instrument equipped with a sensitive quick-response thermopile with a receiver that responds to the entire infrared spectrum should be able to distinguish between a cloud and the clear sky. Such an instrument must also have an optical system to restrict the field of view of the sensitive element to only a small part of the heavens at any instant. The present experimental model of the cloud indicator has the two essential components - a sensitive element and an optical system - mounted in a single housing. This assembly is referred to in the present report as the "thermoelectric eye." The complete cloud indicator also includes an amplifier and an indicating meter. A diagram of an installation of the thermoelectric eye, the amplifier, and the indicating meter on an airplane is shown in figure 1. A cutaway view of the optical system of the thermoelectric eye is given in figure 2. The line of sight may be seen to be elevated slightly above the horizontal.

Because the field of view of the cloud indicator is limited and because a relatively thin layer of cloud surface emits as much radiation as any substance at the same temperature, the response of the cloud indicator is determined in part by the surface temperature of the part of the cloud on which the cloud indicator is sighted. Because some junctions are kept at the housing temperature, the output of the thermopile is partly determined by the housing temperature.

The surface temperature of the part of the cloud sighted on probably approximates closely the temperature of the adjacent clear atmosphere at the same height as the cloud surface; otherwise, convection currents would occur at the surface of the clouds. Whatever convection occurs at the surface is known to be small relative to that at the interior of cumulus clouds. Unpublished data indicate

that interior temperatures of violent cumulus clouds differ by not more than a few degrees from the temperature of the adjacent clear air, and consequently the validity of the statement regarding the relation between the temperature of the cloud surface and that of the adjacent clear atmosphere is established. The atmosphere external to an active cloud, furthermore, is quiescent relative to the activity within the cloud and consequently, as flight measurements have shown, the temperature gradient in a horizontal plane within the surrounding clear atmosphere is small. It is therefore reasonable to assume that the temperature of the cloud surface sighted on is almost the same as the temperature of the clear atmosphere at equal altitude within reasonable distances. The difference in temperature that is partly responsible for the reading of the cloud indicator may therefore be taken as the temperature difference along a vertical passing through the thermoelectric eye. It is known that a temperature gradient of approximately constant value usually exists in the clear atmosphere along vertical lines. This gradient is known to meteorologists as the "lapse rate" of the atmosphere.

The cloud indicator may be calibrated for quantitative estimates of the distance and height of clouds by assuming the validity of the following conditions: (1) The emitting surface of a cloud is at the same temperature as the clear atmosphere of equal altitude within the distance range of the cloud indicator, (2) the temperature gradient of the clear atmosphere is constant in the vertical direction, and (3) the angular elevation of the line of sight is constant. Graduated scales can be provided to take into account the temperature of the clear atmosphere along the flight path. When the elevation of the line of sight remains constant during flight, the slope of the cloud surface sighted on can be estimated from the rate of movement of the indicator and from the speed of the airplane. This slope is important as an indication of the nature of the weather beyond that surface. The cloud indicator therefore is expected to warn the pilot of the existence, approximate location, and probable types of cloud not visible to the unaided eye at night and, as a result, it is expected that storm areas associated with clouds can be avoided by airplanes equipped with this device.

[redacted]

The three conditions assumed in the foregoing discussion represent an ideal simplified case. The actual case is complicated by the following two additional phenomena:

(1) The absorption of the clear atmosphere between the cloud and the thermoelectric eye. This absorption is small in some regions of the spectrum in which atmospheric radiation exists and has given rise to the concept of a "window" in the atmosphere for atmospheric radiation. The absorption elsewhere is, however, far from negligible and consequently must be taken into consideration.

(2) The absorption of the various parts of the thermoelectric eye through which the radiation passes in transit to the receiver of the thermopile. This absorption is not negligible and must also be taken into account. The present analysis of net radiation exchange takes into consideration these two groups of absorption effects and leads to a series of tables and a chart that are useful in calibrating the cloud indicator. Because the three conditions previously listed are not always valid, the cloud indicator cannot be considered a precision instrument.

The symbols used throughout are defined in appendix A.

FACTORS DETERMINING NET RADIATION EXCHANGE

Nocturnal Radiations and Emission of Clouds

At night there are three natural sources of visible light: the moon, the stars and planets, and the "light of the night sky." The illuminations on a horizontal surface due to these sources are given in the following table:

Source of nocturnal illumination	Illumination (meter candle)	Incident radiation relative to change in black-body temperature from 0° C to 1° C
Full moon at zenith (reflected energy only)	0.2	0.3
Starlight	.0009	2.4×10^{-6}
Light of the night sky	.0003	9.0×10^{-7}

[redacted]

The illuminations for the full moon at zenith and for starlight are taken from page 570 of reference 1 and the illumination for the light of the night sky is derived from page 3 of reference 2. By assuming that the spectral distribution of all these sources of visible light has the same distribution as in sunlight and by taking into account the smallness of the angular dimension of the moon relative to the field of view of the cloud indicator, an estimate has been made of the relative intensities of the radiations incident upon the instrument. These estimated incident intensities, relative to the change in intensity produced when the temperature of a neighboring perfect black body on which the instrument is sighting changes from 0° C to 1° C, are also shown in the table.

As may be seen from the table, the starlight and the light of the night sky combined do not appreciably affect the instrument, but the effect of the reflected energy of the full moon is not negligible. Computations based on the thermal radiation emitted by the full moon, with its temperature assumed to be 101° C (reference 3) and with absorption by the intervening atmosphere neglected, indicate that 2.2 must be added to the value of 0.3 given in the table so that the total relative value for the moon is 2.5.

Except when the instrument is sighting directly on the moon, the only radiations from natural sources in the heavens that are intense enough to affect the instrument at night are the invisible thermal emissions. The atmospheric temperatures giving rise to these thermal emissions range from about 200° K to 300° K. Calculations based on Planck's radiation equation show that more than 99 percent of the black-body radiation characteristic of a body at 275° K is in the long-wave part of the spectrum where the wave numbers are less than 2500 per centimeter (2500 cm^{-1}). (Wave number is reciprocal of wave length; therefore 2500 cm^{-1} corresponds to a wave length of 4×10^{-4} cm.) For this reason, only radiations of wave number less than about 2500 cm^{-1} need be considered.

Data on the absorption coefficients (reference 4, pp. 269-270) and spectral transmission (reference 5) for liquid water show that, for the spectral region between 555 cm^{-1} and 2500 cm^{-1}, the over-all transmission factor for black-body radiations characteristic of atmospheric temperatures is less than 0.01 for 0.0060 centimeters or

[redacted]

more of liquid water. It has been reported (reference 6) that clouds have a liquid-water content ranging from 0.5 to 1.5 grams per cubic meter and that higher values probably often occur. For the range of liquid-water content from 0.5 to 1.5 grams per cubic meter, by neglecting the small amount of atmospheric radiation beyond this spectral region and the fact that scattering by the water droplets increases the amount of transmitted radiation, it is concluded that from 40 to 120 meters of cloud having a liquid-water content within this range absorbs at least 0.99 of infrared radiations characteristic of atmospheric temperatures. Because of the effects of scattering, a cloud cannot be assumed to absorb the same fraction of the radiation as an equivalent sheet of water, but experiments indicate that an average cloud 100 meters or more in thickness acts essentially as a black-body absorber in the infrared spectrum. (See reference 7.) With this qualitative experimental check on the blackness of clouds to infrared radiation, it is reasonable to assume that all clouds having a liquid-water content within the range of 0.5 to 1.5 grams per cubic meter and measuring from 40 to 120 meters or more along the line of sight act as almost perfect black-body emitters of infrared radiation. Calibrating an instrument on the basis of perfect emission of clouds consequently is valid for all such clouds except those considerably less than about 100 meters in thickness and those too small to fill completely the field of view of the instrument.

Composition of Clear Atmosphere

The clear atmosphere consists of a number of gases, which exist in almost constant proportions up to altitudes of at least 20 kilometers (reference 8, p. 151). Only about 5 percent of the total mass of air is above this altitude. The nine more abundant atmospheric constituents that exist in constant proportion are given in table I, along with five variable components (references 3 to 10). At least 85 percent of the ozone and nitrogen oxides exist in the stratosphere. (See reference 11.) Since the amount of dust present obviously cannot be specified in the same manner as was used for the gases and the density of the water vapor varies with temperature at a much more rapid rate than the gaseous constituents, the number of grams in a vertical column with a cross section of 1 square centimeter is used, instead of the reduced thickness, in specifying the amount of dust and water

[redacted]

vapor present. The range of values for the water-vapor content of the atmosphere is based upon some observations made at the Mt. Wilson Observatory. (See reference 8, p. 153.) If all the water vapor in a vertical column of the atmosphere given in table I were condensed, it would form a layer over the bottom of the column from 0.5 to 7.0 centimeters deep. The amount of water vapor is stated herein in terms of "centimeters of precipitable water vapor."

In estimating the quantity of dust in the clear atmosphere, only the minute particles of volcanic origin that are always present are considered and the following average values are used:

Number of dust particles in a vertical column 1 cm^2 in cross section above sea level . . . . . 34×10^4

Diameter of dust particles . . . . . 1.85×10^{-4} cm

Density of dust particles . . . . . 2.3 grams/cm^3

These values are taken from reference 1, pages 598, 591, and 593, respectively. The result of the estimate is 3×10^{-6} gram per square centimeter, as given in table I.

Attenuation of Infrared Radiation

By scattering.- Only the molecules of the air and of water vapor produce true scattering. The diameter of these molecules is of the order of 5×10^{-8} centimeter. (See reference 12.) The attenuation of infrared radiation produced by true scattering by the molecules of air and of water vapor has been computed by means of a modified form of Rayleigh's equation for scattering and found to be less than one-tenth of 1 percent for all radiations having a wave number less than about 6230 cm^{-1} (reference 13). Attenuation of the infrared radiation involved in operation of the cloud indicator due to true scattering by the clean air therefore is negligible.

By diffuse reflection.- Particles having diameters of the same order of magnitude as the wave length of the radiation cause diffuse reflection (sometimes referred to as scattering). By use of equation (1)

[redacted]

and figure 1 on page 104 of reference 7 for the attenuation by large particles and of the estimated values given for the size and number of dust particles, the net transmission for all wave numbers from 500 to 2500 cm^{-1} is found to be in excess of 0.998. Attenuation by the dust of the clear atmosphere therefore is also concluded to be negligible.

Absorption by Atmosphere

It is known that none of the monatomic or diatomic gases of the atmosphere (table I) are responsible for any significant part of the emission or absorption by the atmosphere of any infrared radiation of wave number less than 2500 cm^{-1}. The principal constituents of the atmosphere that contribute to the emission and absorption therefore are carbon dioxide, nitrogen monoxide, nitrogen pentoxide, ozone, and water vapor. Each of these five substances has one or more absorption bands in the region from 500 to 2500 cm^{-1}. A preliminary investigation revealed that all but five of these absorption bands are either so weak that they are negligible in comparison with the stronger bands or their effect is masked by other constituents which absorb much more strongly in the same spectral region. These five remaining bands are due to carbon dioxide, ozone, and water vapor.

Carbon dioxide.- The only carbon-dioxide absorption bands of any significance in the present work are those centered at about 667 and 2320 cm^{-1}. From reference 14, the transmission by carbon dioxide in the 2320 cm^{-1} band may be seen to be

Reduced thickness of carbon dioxide (cm)	Transmission factor
0.024	0.71
.3	.45
7	.12
33	.10

[redacted]

The absorption remains constant as the carbon-dioxide content increases beyond 33 centimeters (reference 14). More recent data (see table I of reference 15), however, show that within the band from 2220 to 2500 cm^{-1} the absorption is 100 percent for 220 centimeters at standard temperature (0° C) and pressure (1013 mb). The data of references 14 and 15 were combined in figure 3, which is used to evaluate certain quantities for the present analysis.

More data are available on the 667 cm^{-1} absorption band of carbon dioxide. The spectral transmission factor τ_c can be represented by (see equation (2) of reference 16)

$$\tau_c = \frac{1}{1 + Ku_c} \qquad (1)$$

where

K Callendar's "spectral absorption coefficient" (see fig. 4)

u_c quantity of carbon dioxide at standard pressure and temperature, centimeters

A smooth faired curve has been substituted for the irregular curve of reference 16. This faired curve, shown in figure 4, was then used in computing by equation (1) the transmission factor τ_c for each of several thicknesses of carbon dioxide. The values so computed are shown in figure 5.

The effect of pressure upon transmission by carbon dioxide can be computed by the method described in the section entitled "Water vapor."

Ozone.- The absorption band due to ozone is shown in figure 6, which represents the transmission of solar radiation by the atmosphere, containing 0.21 centimeter of precipitable water vapor. The zenith distance of the sun was such as to make the air mass traversed 1.5 times the air mass along the vertical. The dip in the curve, which extends from about 980 to 1100 cm^{-1}, is principally attributed to ozone. The absorption outside the ozone band is caused by water vapor. Because of the narrowness

[redacted]

of the ozone band, its moderate intensity, and the fact that only about 15 percent of the ozone is in the troposphere, the effect of ozone upon the response of the instrument is estimated to be negligible when the instrument is sighted on clouds.

Water vapor.- The data of Adel and Lampland on atmospheric transmission (reference 17) show that the water-vapor spectrum contains a large number of absorption lines. These closely spaced weak lines are illustrated by the small dips in figure 6. The abrupt dip in the curve at high wave numbers, however, is attributed to the very strong water-vapor band centered at about 1590 cm^{-1}. The fact that the curve does not indicate complete transparency at any wave number is probably due in part to the water-vapor band centered at about 200 cm^{-1}, which is so powerful that its effect is apparent even as far as 2500 cm^{-1}.

The spectral transmission factors of water vapor may be readily determined by making use of two graphs presented by Elsasser (reference 18, pp. 43 and 57). In evolving these graphs, Elsasser smoothed over the small dips in the water-vapor spectrum and made use of the data of Adel and Lampland (reference 17), Fowle (reference 14), Strong (reference 19), and Randall and others (reference 20). The effect of temperature upon the transmission factor within the range of atmospheric temperatures is believed to be small (reference 18, pp. 47 and 48). One of the two graphs by Elsasser (reference 18, p. 57) shows the generalized absorption coefficient plotted against wave number and is reproduced herein in a modified form as figure 7. The modification consists in using only one curve to cover all temperatures within the atmospheric range and is justified by the smallness of the temperature effect and by the uncertainty of the temperatures tentatively assigned by Elsasser to the three curves given on page 57 of reference 18.

The pertinent part of the other graph by Elsasser (reference 18, p. 43) is reproduced as figure 8. By use of figures 7 and 8, the transmission factor for water vapor at any part of the spectrum between 300 and 2100 cm^{-1} can be estimated. Elsasser (reference 18, p. 22) also shows that, insofar as transmission by the water vapor of the atmosphere is concerned, the variation with total pressure can be taken into account by use of a "reduced specific moisture"

[redacted]

$$q\sqrt{\frac{p}{p_{SL}}}$$

where

q actual specific humidity of atmosphere; ratio of density of water vapor to density of moist air

p actual pressure of atmosphere

p_{SL} standard pressure at sea level

The reduced amount of water vapor in the atmosphere between two levels where the pressures are p_0 and p_1 is then

$$u_w = \frac{1}{g}\int_{p_1}^{p_0} q\sqrt{\frac{p}{p_{SL}}}\,dp \qquad (2)$$

where g is acceleration of gravity (980 dynes/gram).

Absorption by Optical System of Thermoelectric Eye

The radiation exchanged between the cloud and the receiver must traverse the lens unit, the air within the housing between the lens unit and the receiver, and the window of the thermopile housing. (See fig. 2.) In the section "Analysis" the net exchange of radiation is determined partly by the over-all spectral transmission factor τ_t (which includes reflection as well as absorption effects) of the entire optical path within the thermoelectric eye and is shown (equation (9)) to be

$$\tau_t = C\tau_L'\tau_a\tau_W'$$

where the subscripts L, a, and W refer to the lens unit, the housing air, and the thermopile window,

[redacted]

respectively, prime indicates that reflection effects are not taken into account, and C is a factor that allows for reflection effects. The spectral transmission factor τ_L' is first evaluated.

Lens unit.- The lens of the experimental model of the cloud indicator is of rock salt and is double convex with spherical surfaces. The dimensions are as follows:

Thickness at center, centimeters	1.62
Radius of curvature, centimeters	6.81
Diameter of effective aperture, centimeters	5.50

The outer surface of the lens is covered with sheet Pliofilm 0.0043 centimeter thick bound to the rock salt with a thin coating of asphalt varnish of high transparency to infrared radiation.

In use, the rays are incident upon the lens at an angle of about 15° with the optic axis of the lens. (See figs. 1 and 2.) For simplicity, however, computations for the transmission factor of the lens were made for incident rays parallel to the optic axis. The error due to this simplification is estimated to be less than 1 percent. For monochromatic radiation, the transmission factor of the lens unit is computed by

$$\tau_L' = \tau_S'\tau_P' \tag{3}$$

where the subscripts L, S, and P refer to the lens unit and its rock-salt and Pliofilm components, respectively. Equation (3) is not exact because τ_S' does not vary exponentially with thickness.

The transmission factor of the rock salt is computed by

$$\tau_S' = \frac{\int_0^R Ie^{-k_S u_S (2\pi r)}\, dr}{\int_0^R I(2\pi r)\, dr} = \frac{2}{R^2}\int_0^R e^{-k_S u_S r}\, dr \tag{4}$$

[redacted]

where

I spectral intensity of incident radiation

k_S spectral-absorption coefficient of rock salt (reference 4, p. 270)

u_S length of path through rock-salt lens, measured along refracted path (function of r)

r radius of elemental ring

R radius of lens aperture

Equation (4) shows the actual variation of τ_S' with thickness. The deviation of τ_S' from an exponential variation with thickness, however, is small and equation (3) is therefore valid for practical purposes.

The net transmission factor of the Pliofilm component is computed by

$$\tau_P' = e^{-k_P u_P} \qquad (5)$$

where

k_P absorption coefficient of Pliofilm estimated from Well's data (reference 21)

u_P thickness of Pliofilm sheet

In estimating k_P from Well's data, allowance was made for reflection by assuming that at the two surfaces the intensity transmitted was diminished 10 percent by this effect. Well's data were obtained with finite slit widths and consequently the transmissions reported are not true monochromatic values. Since the difference in thickness between the specimen of reference 21, which was 0.0030 centimeter thick, and the one used in the present analysis is small, the error resulting from the use of equation (5) is also small.

Housing air and thermopile window.- The average path length through the air inside the thermoelectric eye is 6.73 centimeters. The amount of precipitable water vapor along this path under the most humid conditions to be

[redacted]

encountered in practice is estimated to be about 0.0001 centimeter, and the amount of carbon dioxide along this same path is estimated to be about 0.0020 centimeter at standard temperature and pressure. Figures 7 and 8 show that the transmission factor of the water-vapor content is almost unity for all parts of the spectrum of interest here. By referring to figures 3 and 5, it is apparent that the carbon-dioxide content has a transmission factor of at least 0.995 for all pertinent wave numbers. For all practical purposes, therefore, τ_a is unity.

The average path length through the window of the thermopile is estimated to be 0.26 centimeter. By use of the values of spectral absorption coefficients listed on page 270 of reference 4, the spectral transmission factors for the window τ_w are computed by an equation of the same form as equation (5).

Optical path within thermoelectric eye.- The numerical values of the spectral transmission factors for the three parts of the optical path are multiplied together to obtain the spectral transmission factors of the entire optical system within the thermoelectric eye. The results of these computations are shown in figure 9. A factor C of 0.9 is used to approximate the over-all effect of reflection at the surfaces of the lens unit and of the thermopile window.

ANALYSIS

The net exchange of radiation at the receiver of the thermopile when the device is sighting on a cloud is seen to be determined primarily by the following parameters:

(1) Thermal emission by receiver of thermopile

(2) Thermal emission of cloud

(3) Absorption and emission by water vapor and carbon dioxide in atmosphere along line of sight

(4) Absorption and emission by rock salt and Pliofilm of lens unit

[redacted]

In addition to the foregoing parameters, others of secondary importance are

(5) Absorption and emission of relatively dry air within main housing

(6) Absorption and emission of rock-salt window of the thermopile housing

All these parameters are determined partly by the temperatures of the various materials involved.

The analysis therefore consists in first setting up an equation for the net exchange of radiation in terms of the individual emissions and absorptions. This equation is then reduced to the minimum number of terms and a general equation is derived for monochromatic atmospheric radiation. In deriving this general equation, the atmosphere is assumed to be homogeneous in any horizontal plane. No assumption is made concerning the distribution of temperatures or humidity along the vertical. The general equation is then multiplied by the spectral transmission factor of the optical path within the thermoelectric eye and integrated over the entire spectrum. A modified form of this equation is developed that leads to a practical solution of the radiation-exchange problem.

Net Exchange of Radiation between Receiver and Atmosphere

The first step in setting up an equation for the net exchange of radiation flux ΔF between the receiver of the thermopile and the cloud, as modified by the intervening atmosphere and parts of the thermoelectric eye, is to write an equation in terms of the six parameters previously listed. By letting ΔF be the net loss of flux by the receiver, this equation obviously is

$$\Delta F = F_R - F_W - F_a - F_L - F_A - F_C \qquad (6)$$

where

F_R emission by receiver of thermopile

F_W emission by window of thermopile

[redacted]

F_a emission by air within main housing modified by losses in window

F_L emission by lens unit modified by losses in housing air and window

F_A radiation emerging from surface of atmosphere in contact with lens, due to self-emission by atmosphere modified by losses in lens unit, housing air, and window

F_C emission by part of cloud (or other body) sighted on modified by losses in atmosphere, lens unit, housing air, and window

and each term represents the flux in the radiation beam having boundaries determined by the lens unit and the receiver of the thermopile. (See fig. 2.) For convenience, each term of equation (6) is expressed in terms of an equivalent flux in the part of the same beam outside the thermoelectric eye that is incident upon the lens unit. A common unit for all terms of equation (6) might be watts per square centimeter of the aperture area within the solid angle of the field of view of the thermoelectric eye.

In the present cloud indicator, the field of view corresponds to a conical half-angle of about $2\frac{1}{4}^\circ$ at the thermoelectric eye. In appendix B the transmission factors of conical beams with half-angles less than 4.5° are shown to differ by less than 1 percent from the transmission factors for parallel beams when all other conditions are the same. For present purposes, therefore, parallel-beam transmission factors can be used in the analysis involving the equivalent beams outside the thermoelectric eye.

Since parallel-beam transmission factors vary exponentially with the thickness of the absorbing substance (that is, $\tau = e^{-ku}$), it therefore follows that when such transmission factors are used, and only when these are used, the over-all transmission factor of the entire optical path can be calculated by taking the product of the individual transmission factors.

The effect of the size of the field of view is taken into account in the analysis by use of the factor $\pi \sin^2\theta$, which appears in equation (B1) of appendix B.

[redacted]

Another simplification can be made in the analysis by assuming the following ideal conditions for the thermoelectric eye, which are valid in the normal use of the device:

(1) All parts of the main housing and all components within it are at a uniform temperature.

(2) All interior surfaces of the thermoelectric eye exposed to view of the thermopile receiver, except those within the cone defined by the lens unit, are perfect black-body radiators.

For the present, it is also assumed that there are no losses due to reflection. The right-hand side of equation (6) then becomes

$$\int_0^\infty \left(f_R - \epsilon_W f_R - \epsilon_a f_R \tau_W' - \epsilon_L f_R \tau_W' \tau_a' - f_A'' \tau_W' \tau_a' \tau_L' - f_C'' \tau_W' \tau_a' \tau_L'\right) d\upsilon \qquad (7)$$

where

f flux of monochromatic radiation for conditions previously specified for the various F-quantities

τ' transmission factor of parallel-beam monochromatic radiation, not including reflection effects

ϵ emission factor corresponding to $\tau(1 - \tau')$

The double prime indicates no modification by the lens unit, housing air, and window, and the subscripts refer to the same bodies as before.

Expression (7) can then be regrouped and simplified as

[redacted]

$$\int\left\{f_R\left[1 - \left(1 - \tau_W'\right) - \left(1 - \tau_a'\right)\tau_W' - \left(1 - \tau_L'\right)\tau_W'\tau_a'\right]\right.$$

$$\left. - f_A''\tau_W'\tau_a'\tau_L' - f_C''\tau_W'\tau_a'\tau_L'\right\} d\upsilon$$

$$= \int \tau_W'\tau_a'\tau_L'\left(f_R - f_A'' - f_C''\right) d\upsilon$$

which does not take into consideration the effect of losses by reflection. In order to allow for the effect of reflection, a reflection function can be introduced. This function is almost independent of wave number between 2500 and 500 cm^{-1} and consequently a constant factor C can be put in equation (6) to allow for reflection losses. Equation (6) then may be written

$$\Delta F = \int \tau_t f_R \, d\upsilon - \int \tau_t f_A'' \, d\upsilon - \int \tau_t f_C'' \, d\upsilon \qquad (8)$$

where

$$\tau_t = C\tau_W'\tau_a'\tau_L' \qquad (9)$$

and represents the over-all spectral transmission factor of the entire optical path within the thermoelectric eye. Each term on the right-hand side of equation (8) has the transmission factor τ_t as a common factor. Because of this fact, a general equation for self-emission of the atmosphere as transmitted by the thermoelectric eye is first derived.

[redacted]

General Equation for Self-Emission of Atmosphere as Transmitted by Thermoelectric Eye

There are two important selectively emitting constituents in the atmosphere, namely, water vapor and carbon dioxide. Assume an atmosphere composed of these two self-emitting constituents, water vapor and carbon dioxide, and denote them by the subscripts w and c, respectively; assume further that the atmosphere is homogeneous in any horizontal plane and that temperature and composition vary with changes in altitude. Figure 10 is a diagram of a horizontal slab of such an atmosphere.

Let du_w be the amount of water vapor and du_c be the amount of carbon dioxide in an elemental layer of unit cross-sectional area. The monochromatic-radiation intensity emitted in the direction θ (fig. 10) is

$$I_{b_N} k_w \sec\theta \, du_w + I_{b_N} k_c \sec\theta \, du_c$$

where k_w and k_c are the absorption (or emission) coefficients and I_{b_N} is the intensity of monochromatic radiation in the normal direction emitted by a perfect black body.

The transmission factor of the part of the slab below the elemental sheet is

$$e^{-k_w u_w \sec\theta - k_c u_c \sec\theta}$$

The monochromatic intensity emerging from the bottom surface of the slab of atmosphere in the direction θ therefore is

$$I_A'' = \int_{u_{w_0}, u_{c_0}}^{u_{w_1}, u_{c_1}} e^{-(k_w u_w + k_c u_c)\sec\theta} I_{b_N} \sec\theta \, (k_w \, du_w + k_c \, du_c) \tag{10}$$

[redacted]

Let f_A'' be the radiant flux emerging from the bottom surface within the cone of half-angle θ. Then

$$f_A'' = 2\pi \int_0^{\theta} I_A'' \sin\theta \cos\theta \, d\theta$$

$$= 2\pi \int_{u_{w_0}, u_{c_0}}^{u_{w_1}, u_{c_1}} I_{b_N} (k_w \, du_w + k_c \, du_c) \int_0^{\theta} e^{-(k_w u_w + k_c u_c)\sec\theta} \sin\theta \, d\theta \tag{11}$$

The transmission factor τ_A of a slab for monochromatic radiation of conical half-angle θ is derived as equation (B3) in appendix B. Equation (B3), when adapted to this slab, is

$$\tau_A = \frac{2}{\sin^2\theta} \int_0^{\theta} \cos\theta \sin\theta \, e^{-(k_w u_w + k_c u_c)\sec\theta} \, d\theta \tag{12}$$

For any particular atmosphere, u_c is a function of u_w, so $u_c = u_c(u_w)$

Then

$$\frac{\partial \tau_A}{\partial u_w} = \frac{2}{\sin^2\theta} \int_0^{\theta} - \left[k_w + k_c \frac{du_c(u_w)}{du_w} \right] \sin\theta \, e^{-\left[k_w u_w + k_c u_c(u_w)\right]\sec\theta} \, d\theta \tag{13}$$

Also, the expression within the first parentheses of equation (11) may be written as

$$k_w \, du_w + k_c \frac{du_c(u_w)}{du_w} du_w$$

[redacted]

Therefore

$$f_A'' = - \pi \sin^2\theta \int_{u_{w_0}}^{u_{w_1}} I_{b_N} \frac{\partial \tau_A}{\partial u_w} du_w \qquad (14)$$

From appendix B, however,

$$\pi I_{b_N} \sin^2\theta = f_b$$

where f_b is the black-body flux within the cone of half-angle θ. Therefore

$$f_A'' = \int_{u_{w_1}}^{u_{w_0}} f_b \frac{\partial \tau_A}{\partial u_w} du_w \qquad (15)$$

If τ_t is the over-all transmission factor of the thermoelectric eye for conical-beam radiation of half-angle θ, the self-emission of the atmosphere of all wave numbers υ and within the cone of half-angle θ and transmitted by the thermoelectric eye is

$$F_A = \int_0^\infty \tau_t f_A'' \, d\upsilon$$

$$= \int_0^\infty \tau_t(\upsilon,\theta) \, d\upsilon \int_{u_{w_1}}^{u_{w_0}} f_b(T,\upsilon,\theta) \frac{\partial \tau_A(u_w,u_c,\theta,\upsilon)}{\partial u_w} du_w \qquad (16)$$

where the absolute temperature T is a function of u_w.

[redacted]

For a given instrument the field of view, and therefore θ, is fixed; consequently, θ in equation (16) is considered constant. Also, use is made of the fact that, for all fields of view of the size contemplated for the cloud indicator, the transmission factors are almost the same as for parallel beams. (See appendix B.) Equation (16) therefore may be written

$$F_A = \int_0^{\infty} \tau_t(\upsilon)\, d\upsilon \int_{u_{w_1}}^{u_{w_0}} f_b(T,\upsilon)\, \frac{\partial \tau_A(u_w,u_c,\upsilon)}{\partial u_w}\, du_w \qquad (17)$$

Equation (17) is the general equation for self-emission of the atmosphere as transmitted by the thermoelectric eye.

Modified Form of General Equation Leading to a Practical Radiation Chart

Evaluation of F_A by direct application of equation (17) would involve a point-by-point double integration. A modification of equation (17) that greatly facilitates this evaluation can be made by a method which closely follows the method of Elsasser (reference 18, pp. 19-20). The first step in the modification consists of integrating by parts the second integral of equation (17) as follows:

$$\int_{u_{w_1}}^{u_{w_0}} f_b(u_w,\upsilon)\, \frac{\partial \tau_A(u_w,u_c,\upsilon)}{\partial u_w}\, du_w$$

$$= f_b(u_w,\upsilon)\, \tau(u_w,u_c,\upsilon)\Big]_{u_{w_1}}^{u_{w_0}} - \int_{f_{b_1}(u_{w_1})}^{f_{b_0}(u_{w_0})} \tau_A(u_{w_1},u_c,\upsilon)\, df_b(u_w,\upsilon) \qquad (18)$$

[redacted]

where

$$df_b(u_w,v) = \frac{\partial f_A(u_w,v)}{\partial u_w} du_w \tag{19}$$

Since u_w is a function of T, equation (19) may be written

$$df_b(u_w,v) = \frac{\partial f_A(T,v)}{\partial T} dT \tag{20}$$

and equation (17) therefore becomes

$$F_A = \int_0^\infty \tau_t(v)\, f_b(T,v)\, \tau_A(u_w, u_c, v)\, dv \Bigg]_{u_{w_1}}^{u_{w_0}} - \int_{T_1(u_{w_1})}^{T_0(u_{w_0})} dT \int_0^\infty \tau_t(v)\, \frac{\partial f_b(T_1,v)}{\partial T}\, \tau_A(u_w,u_c,v)\, dv \tag{21}$$

Let

$$\int_0^\infty \tau_t(v)\, \frac{\partial f_b(T,v)}{\partial T}\, \tau(u_w,u_c,v)\, dv = Q(u_w,u_c,T) \tag{22}$$

The quantity Q, which is defined by equation (22), is fundamental. The evaluation of Q is briefly outlined in appendix C. For any particular atmosphere, in which u_c is a function of u_w, the second term of equation (21) therefore becomes the line integral

$$\oint_{u_{w_1},T_1}^{u_{w_0},T_0} Q(u_w,T)\, dT$$

[redacted]

In order to convert the first term of equation (21) to a form similar to that of the last term, consider the first term with the upper limit, make use of the fact that T is a function of u_w, and again drop u_c, because for any particular atmosphere u_c is a function of u_w. Both u_w and u_c can be computed from radiosonde data. Each is a function of altitude and of temperature and consequently one can be expressed as a function of the other. Then

$$\int_0^\infty \tau_t(\upsilon)\ f_b(T,\upsilon)\ \tau(u_w,u_c,\upsilon)\ d\upsilon \Bigg]^{u_{w_0}}$$

$$= \int_0^\infty \tau_t(\upsilon)\ f_b(T_0,\upsilon)\ \tau_A\left(u_{w_0},\upsilon\right) d\upsilon \qquad (23)$$

But

$$f_b(0,\upsilon) = 0$$

The first term with the upper limit therefore may be written

$$\int_0^\infty \tau_t(\upsilon) \left[f_b(T_0,\upsilon) - f_b(0,\upsilon) \right] \tau_A\left(u_{w_0},\upsilon\right) d\upsilon$$

$$= \int_0^{T_0} dT \int_0^\infty \tau_t(\upsilon) \frac{\partial f_b(T,\upsilon)}{\partial T} \tau\left(u_{w_0},\upsilon\right) d\upsilon$$

$$= \int_0^{T_0} Q\left(u_{w_0},T\right) dT \qquad (24)$$

The first term of equation (21) with the lower limit likewise becomes

$$\int_0^{T_1} Q\left(u_{w_1},T\right) dT$$

[redacted]

and equation (17) may therefore be written

$$F_A = \int_0^{T_0} Q\left(u_{w_0}, T\right) dT - \int_0^{T_1} Q\left(u_{w_1}, T\right) dT - \int_{u_{w_1}, T_1}^{u_{w_0}, T_0} Q\left(u_{w_1}, T\right) dT \tag{25}$$

Finally, if $u_{w_0} = 0$ and $u_{w_1} = U_w$ and the terms are rearranged,

$$F_A = \int_0^{T_0} Q(0,T)\, dT + \oint_{T_0, u_{w_0}}^{T_1, u_{w_1}} Q(u_w, T)\, dT + \int_{T_1}^{0} Q(U_w, T)\, dT \tag{26}$$

The path of integration on a QT-plane is a closed figure, the area of which represents the radiant flux transmitted by the thermoelectric eye due to self-emission in the atmosphere. If T_0 is the temperature of the receiver of the thermopile and T_1 is the temperature of the cloud, it is obvious that F_A also represents the second term of equation (8) $\int \tau_t f_A'' \, d\upsilon$.

A Radiation Chart Adapted to Cloud Indicator

Equation (26) takes into account both carbon dioxide and water vapor. For any one atmosphere, in which the quantity of carbon dioxide is a function of water vapor, a chart can be constructed with Q and T as axes, from which the radiation transmitted by the thermoelectric eye can be determined for that atmosphere; that is, each atmosphere can be represented by a radiation chart. Figure 11 illustrates the type of closed curve defined by equation (26) plotted on a QT-plane. In figure 11 T_0 is the temperature of the receiver of the thermopile

[redacted]

and T_1 is the temperature of the cloud. The atmosphere is represented by the line immediately under area B. The significance of the various areas on this chart is as follows:

Area A + B.- As has been stated area A + B represents the second term of equation (8) $\int \tau_t f_A'' \, d\upsilon$.

Area A.- Area A represents self-emission of an isothermal atmosphere containing U_w centimeters of precipitable water vapor and $u_c(U_w)$ centimeters of carbon dioxide at a temperature T_1, as transmitted by the thermoelectric eye.

Area A + D.- Area A + D represents the self-emission of a black body at a temperature T_1 transmitted by the thermoelectric eye.

Area D.- Area D represents the black-body emission characteristic of temperature T_1 transmitted by the atmosphere containing U_w centimeters of precipitable water vapor and $u_c(U_w)$ centimeters of carbon dioxide and by the thermoelectric eye. This area therefore represents the third term of equation (8) $\int \tau_t f_C'' \, d\upsilon$.

Area A + B + C + D.- Area A + B + C + D represents the self-emission of a black body at a temperature of T_0, transmitted by the thermoelectric eye. This area therefore represents the first term of equation (8) $\int \tau_t f_R \, d\upsilon$.

By equation (8), the exchange of radiant flux at the receiver of the thermopile ΔF is therefore given by

$$\Delta F = (A + B + C + D) - (A + B) - D$$

$$= C \qquad (27)$$

[redacted]

This area C is the line integral represented by the second term of equation (26) or in more concise form by

$$C = \int_{T_1}^{T_0} Q \, dT \tag{28}$$

Preliminary computations show that, for the range of atmospheric temperature and atmospheric content of water vapor and carbon dioxide expected in flight use of the cloud indicator, the relative values of $Q(u_w,u_c,T)$ range from 1 to 2000. The variation of Q with each parameter, while the other two are held constant, is so great that numerous tables or families of curves would be needed to represent the values of Q within reasonable tolerances. In order to avoid the necessity of using a great number of tables or families of curves, a plane different from that used for figure 11 is used for the radiation chart.

Let the coordinates of the new plane be y and x, where

$$\int y \, dx = \int Q \, dT \tag{29}$$

in which $Q = Q(u_w,u_c,T)$, as defined in equation (22), and y is an arbitrary constant y_0 for $u_c = 0$ and $u_w = 0$. Also let

$$x = \int \frac{Q(0,0,T)}{y_0} \, dT$$

$$\equiv x(T) \tag{30}$$

When equations (29) and (30) are combined,

$$y = \frac{Q(u_w,u_c,T)}{Q(0,0,T)} \, y_0$$

$$\equiv y(u_w,u_c,T) \tag{31}$$

The yx-plane that is used in constructing the radiation chart is defined by equations (30) and (31). The variation of y with T, as u_w and u_c are held constant, is found to be so small that five tables are sufficient to represent within a small tolerance the values of y for any combination of u_w, u_c, and T expected in flight use.

RESULTS

Values of y (equation (31)) have been computed for the limiting quantities of water vapor, carbon dioxide, and temperature expected during use of the cloud indicator in flight. These values of y, along with others for some intermediate flight quantities, are plotted in figure 12 in which y_0 has been arbitrarily assigned a value of 100. The nonuniform temperature scale of figure 12 results from using x(T) of equation (30) for the abscissa.

Figure 12 shows that, for the majority of combinations of water vapor and carbon dioxide, the variation of y with temperature is small. The curves for $u_w = 0$ and $u_c = 550$ and for $u_w = 1$ and $u_c = 0$ show the greatest variation - about 15 percent of the maximum ordinate of 100. Further computations of y show that the maximum variation of y with temperature occurs for a combination of about 0.25 centimeter of precipitable water vapor and no carbon dioxide. For this combination, the variation of y with temperature is shown in figure 13. The maximum variation for this case is found to be ±9 percent of the maximum ordinate.

The percentage variation with temperature can be made smaller than any desired value by dividing the temperature scale into sufficiently small intervals. For each of these intervals, a table can be made which gives a value of y for any specified combination of water vapor and carbon dioxide and is valid throughout that temperature range within any desired tolerance. The number of tables giving values of y is determined by the accuracy required. For present purposes, it is estimated that tables covering temperature ranges in which the variation of y with temperature is no more that ±2 percent can be tolerated. Five such tables are therefore needed.

[redacted]

An inspection of figure 13 indicates that the total variation is divided into five approximately equal parts with a maximum variation of ±1.8 percent by the five temperature ranges in the following table:

Range in temperature (°K)	Representative temperatures (°K)	Table
213 to 235	224	II
235 to 256	245	III
256 to 282	267	IV
282 to 299	289	V
299 to 323	311	VI

Figure 13 also indicates that representative values of y for each of these five intervals can be obtained at the temperatures given in the middle column of the table. For each of the five temperatures given in the middle column, evaluations are made of the quantity y (equation (31)) for numerous combinations of water-vapor and carbon-dioxide content. Some details of these evaluations are given in appendix C. The result of these evaluations are presented in tables II to VI, in which all temperatures are expressed, for the user's convenience, in degrees Centigrade.

For convenience in plotting y against temperature in such a manner that the area under the curve is a measure of the net exchange of radiation at the receiver of the thermopile, a plane is ruled (fig. 14) with uniformly spaced horizontal lines for directly plotting as ordinates values of y from the tables and with a nonlinear abscissa scale (divided according to equation (30)) for plotting temperatures. For the experimental model of the cloud indicator, the area scale is such that the entire ruled area of figure 14 represents $6560\pi \sin^2\theta$ microwatts of radiation per square centimeter of lens aperture.

Elsasser states on page 57 of reference 18 that not much is known about the accuracy of the individual

[redacted]

measurements upon which the generalized absorption coefficients are based. This fact, combined with a further loss of accuracy as a result of the smoothing process involved in Elsasser's generalized absorption coefficient, precludes any claim for high accuracy in the results obtained by the analysis when figure 7 is used to determine the transmission factor of water vapor. Any definite statement concerning the over-all accuracy of the values given in tables II to VI therefore is impossible. When the experimental setup is such as to satisfy the conditions that were assumed in making the analysis, however, it seems reasonable to expect that the probable over-all error in integrated radiation exchange obtained by means of the tables and chart will not be large, probably not greater than about 5 percent for many combinations of the independent variables.

DISCUSSION

The tables that have been developed for the cloud indicator can also be used for any similar infrared device provided that the angular extent of the beam, both within and without the thermoelectric eye, is not much greater than in the present device and provided that the spectral transmission factors are essentially the same as for the present device. The second specification effectively limits the use of the present tables to similar devices that contain a lens unit of rock salt and Pliofilm and have average thicknesses about the same as in the present device. The lens, however, may have different dimensions, and therefore different speeds and different fields of view, provided that the foregoing specifications are fulfilled. Similar tables could be constructed for similar infrared devices that do not conform to the foregoing specifications.

The radiation chart (fig. 14) has the same validity and limitations as the tables. Similar charts could also be constructed for similar infrared devices.

The tables and the chart can be used to determine the exchange of radiation between the receiver of the cloud indicator and any black-body radiator including, for example, any blackened surface of known temperature that might be used in calibration.

[redacted]

The tables and chart for calibrating the cloud indicator are valid for a clear atmosphere with the normal complement of minute dust particles. The larger dust particles and haze are known to affect markedly the net exchange of radiation, but these effects are not considered in the present analysis because no practical flight method of readily determining the density of either of these constituents in the atmosphere is known. This omission, however, appears not serious for the cloud indicator when used as contemplated by trans-ocean transport airplanes because under such flight conditions the occurrence of haze, and especially of large dust particles, is not frequent.

Calibration of the cloud indicator is greatly simplified by means of the tables and the radiation chart. Without these aids, the determination would involve a point-by-point double integration over the spectrum and over the range of altitude or of some parameter defined by altitude.

The area under a curve that represents the intervening atmosphere, on either a QT- or yx-plane, represents the exchange of radiation at the receiver in terms of the field of view of the cloud indicator. The accuracy with which the effective field of view is known consequently determines, in part, the over-all accuracy of the determination. Errors due to faulty values of the effective field of view, as well as to the use of parallel-beam transmission factors, however, can be largely eliminated by a direct calibration made by sighting the device directly on a nearby black body at known temperature.

The present analysis and the resulting tables and chart are directly applicable to conical beams of radiation with their center lines perpendicular to homogeneous slabs of the atmosphere and hence may be applied directly to the cloud indicator when it is sighted vertically upward. For all practical purposes, the same tables and chart can be used when the device is not sighted vertically by using, as the quantity of absorber sighted through, the amount along the center line of the inclined line of sight rather than the quantity along the vertical. This procedure obviously is not entirely accurate because rays that constitute a hollow cone about the center line of the field of view in this case do not traverse paths with identical characteristics. The errors introduced

[redacted]

by the rays above the center line, however, tend to compensate for the errors introduced by the rays below the center line and, consequently, since the field of view of the cloud indicator is small (about $4\frac{1}{2}^{\circ}$), the error introduced by this simplifying assumption is small - probably not more than a few percent. The analysis and the resulting equation (equation (26)) are exact. The transmission factors appearing in this equation, however, are the values for conical beams of monochromatic radiation and for the spatial distribution of energy that actually exists; that is, an error, though usually small, is introduced in any numerical computation that uses transmission factors for parallel beams traversing slabs with parallel surfaces and for finite spectral intervals. Two examples of the way in which the tables and chart can be used in determining the radiation exchange when the cloud indicator is sighted either toward the zenith or in some other direction are given in appendix D.

CONCLUSIONS

An experimental model of a cloud indicator, which is a flight instrument utilizing infrared radiations for detecting and indicating the location of clouds at night, has been developed. The preliminary investigation, based upon data in the scientific literature, of the factors that might determine the exchange of radiation between the receiver of the cloud indicator and a cloud, indicated the following conclusions:

1. Except when the cloud indicator is sighting directly on the moon, the only radiation from natural sources in the heavens that are intense enough to affect the readings of the instrument are the thermal emissions in the infrared region of the spectrum.

2. Clouds of moderate thickness are almost perfect thermal emitters of infrared radiations.

3. Attenuation of infrared radiation emitted by clouds due to scattering by molecules of the atmosphere or to diffuse reflection by the normal complement of dust particles in the atmosphere is negligible.

[redacted]

4. Water vapor and carbon dioxide are the only constituents of the clear atmosphere that are important in modifying the exchange of radiation.

The analysis of the exchange of radiation given in the present paper indicated the following conclusions:

5. A practical means has been provided for determining the exchange of radiation between the receiver of the cloud indicator and a cloud as modified by emission and absorption of the intervening atmosphere and by the selectively absorbing parts of the thermoelectric eye. The determination takes into account the effect of the carbon-dioxide content as well as the water-vapor content of the atmosphere.

6. The tables and the radiation chart presented are expected to serve as a valid guide in extrapolating results of field observations made with the cloud indicator to cover all probable flight conditions. They should therefore aid in devising a practical scale for the cloud indicator for use in flight.

Langley Memorial Aeronautical Laboratory
National Advisory Committee for Aeronautics
Langley Field, Va.

[redacted]

APPENDIX A

SYMBOLS

C	reflection constant
C_1	first radiation constant (1.1906×10^{-12} watt cm^2 $steradian^{-1}$)
C_2	second radiation constant (1.4384 cm deg)
f	flux of monochromatic radiation, watt cm^{-2}/cm^{-1}
Δf	net exchange of monochromatic radiation flux, watt cm^{-2}/cm^{-1}
F	total flux of all radiation in spectrum, watt cm^{-2}
g	acceleration of gravity (980 dynes/gram)
h	relative humidity
I	intensity of monochromatic radiation, watt cm^{-2} $steradian^{-1}/cm^{-1}$
k	absorption coefficient, cm^{-1}
K	Callendar's "absorption coefficient" (reference 16)
l	Elsasser's generalized absorption coefficient (reference 18)
m	mixing ratio, gm of water per kg of dry air
P	atmospheric pressure, mb
Q	function defined by equation (22), watt cm^{-2} $(^oK)^{-1}$
r	radius of elemental ring, cm
R	radius of lens aperture, cm
T	absolute temperature, ^oK
u	reduced thickness of absorbing material, cm

[redacted]

U	total reduced thickness of absorbing material in slab of atmosphere, cm
q	specific humidity
x	function of temperature; defined by equation (30)
y	function of carbon-dioxide and water-vapor content and of temperature; defined by equation (31)
ϵ	emission factor
θ	angle with normal to surface, radians or deg
υ	wave number of monochromatic radiation, cm^{-1}
τ	transmission factor

Subscripts:

a	air within housing of thermoelectric eye
A	atmosphere
b	black body
c	carbon dioxide
C	cloud (or other black body sighted on)
L	lens unit of thermoelectric eye
N	normal to surface
p	pressure
P	Pliofilm
R	receiver of thermopile
s	saturated water vapor in atmosphere
S	rock-salt component of lens unit
SL	sea level
t	thermoelectric eye

[redacted]

w water vapor

W window of thermopile

0 specified level in atmosphere or zero quantity of absorbing material

1 another level in atmosphere

Prime indicates that reflection effects are not included. Double prime indicates no modification by lens unit housing air and window.

[redacted]

APPENDIX B

TRANSMISSION OF A DIVERGING BEAM OF MONOCHROMATIC RADIATION

The transmission factor τ' of a horizontal parallel slab of homogeneous absorbing material of thickness u for a parallel beam of monochromatic radiation is given by

$$\tau' = e^{-ku \sec \theta}$$

where

θ angle between incident beam and normal to surface of slab

k absorption coefficient of material of which slab is composed

Assume that a horizontal-plane black-body surface is emitting isotropic diffuse monochromatic radiation into the same slab. Let I_{b_N} be the intensity of the radiation emitted normally to the surface and I_b the intensity in the direction θ with the normal. By Lambert's cosine law

$$I_b = I_{b_N} \cos \theta$$

The total flux of radiation emitted within a cone of half-angle θ is then

$$f_b = 2\pi \int_0^\theta I_{b_N} \cos \theta \sin \theta \, d\theta$$

$$= \pi I_{b_N} \sin^2 \theta \qquad \text{(B1)}$$

[redacted]

Likewise, the total flux transmitted by the slab of thickness u is

$$f_{b_u} = 2\pi \int_0^{\theta} I_{b_N} \cos\theta \sin\theta \, e^{-ku \sec\theta} d\theta \quad (B2)$$

and the transmission factor is

$$\tau_A = \frac{f_{b_u}}{f_b} = \frac{2\int_0^{\theta} \cos\theta \sin\theta \, e^{-ku \sec\theta} d\theta}{\sin^2\theta} \quad (B3)$$

It is apparent that, as θ approaches 0, τ_A approaches e^{-ku}. Furthermore, an evaluation of equation (B3) shows that, for conical beams of half-angle θ less than 4.5°, the difference between the value of τ_A and e^{-ku} is less than 1 percent even when the absorption is great enough to cut the net transmission to less than 0.001 of the incident value; that is, even when ku is as large as 6.9.

[redacted]

APPENDIX C

EVALUATION OF QUANTITY y IN EQUATION (31)

The quantity y in equation (31) can be evaluated only after evaluation of Q in equation (22). The quantity Q involves the term $\frac{\delta f_b}{\delta T}$ which, by equation (B1) becomes $\pi \sin^2\theta \frac{\delta I_{b_N}}{\delta T}$.

By Planck's radiation law

$$I_{b_N} = \frac{c_1 \upsilon^3}{\left(e^{\frac{c_2 \upsilon}{T}} - 1\right)} \qquad (C1)$$

where the values of the radiation constants are

$$c_1 = 1.1906 \times 10^{-12} \text{ watt cm}^2 \text{ steradian}^{-1}$$

and

$$c_2 = 1.4384 \text{ cm deg}$$

These constants were used in the evaluation of $\frac{\delta f_b}{\delta T}$ for various combinations of temperature T and wave number υ.

The expression for Q (equation (22)) also involves the spectral transmission factor of the atmosphere τ_A. For monochromatic radiation

$$\tau_A = \tau_w \tau_c \qquad (C2)$$

where the subscripts w and c indicate the water-vapor and carbon-dioxide contents of the atmosphere, respectively.

[redacted]

Hence, τ_A was computed by equation (C2) with the use of figures 3, 5, 7, and 8. The other factor in the expression for Q is τ_t, for which values were obtained from figure 9.

The integrations over all wave numbers, for each combination of water-vapor and carbon-dioxide content and of temperature, were carried out for all possible combinations of the following values of the three parameters:

Water-vapor content (cm)	Carbon-dioxide content (cm)	Temperature ($^{\circ}$K)
0	0	224
.01	.23	245
.10	1	267
.25	4	289
1	20	311
2.5	100	
5	550	
10		
25		

After Q was computed for each of the combinations, the corresponding values of y were computed by equation (31). An inspection of these values of y showed that graphical representation was not practical and that smaller increments were necessary for tabular representation. The additional values were obtained by a system of plotting and fairing curves and are included in tables II to VI.

[redacted]

APPENDIX D

EXAMPLES OF USE OF RADIATION TABLES AND CHART

A numerical example is given to illustrate the way in which the radiation tables and chart derived in the present report can be used to estimate the net radiation exchange at the receiver of the cloud indicator for purposes of calibration.

The atmosphere used as an example is one that existed at Langley Field, Va. on the evening of October 1, 1943. The values of pressure, temperature, and relative humidity were determined by a radiometeorograph and some of the important results obtained are given in table VII. During the ascent of the radiometeorograph, an overcast with a base height varying from 5600 feet to 7200 feet was observed.

Equation (2), which involves the specific humidity q, is used to compute the amount of water vapor between each of the 14 levels of table VII. Available tables and charts, however, give only the saturation ratio m_s and therefore values of the actual ratio m must be obtained by

$$m = hm_s \qquad (D1)$$

where h is the relative humidity. The corresponding values of specific humidity are then determined by the equation

$$q = m(1 - m) \qquad (D2)$$

which holds to within one-tenth of 1 percent throughout the range of values found in the atmosphere. The values of q thus obtained are also given in table VII.

Standard atmospheric pressure at sea level p_{SL} is 1013 millibars. By using this value, the reduced specific moisture $q\sqrt{\frac{p}{p_{SL}}}$ is computed (column (5),

[redacted]

table VII). Multiplying the mean of this value for any slab between two adjacent layers by the difference in atmospheric pressure and dividing by the acceleration of gravity g gives the quantity of water vapor along the vertical within that slab, as indicated by equation (2). These values are shown in column (8). (It may be noted that 1 mb = 1000 dynes/cm^2; and g = 980 dynes/gram; hence the factor 1/0.980 in column (8).)

In order to compute the quantity of carbon dioxide, use is made of the fact that the percentage composition is constant at all levels involved and hence the amount of carbon dioxide above any level is proportional to the pressure at that level. When the total carbon-dioxide content of the atmosphere is taken to be 240 centimeters at standard pressure and temperature (table I), the amount of carbon dioxide along the vertical above that level is

$$u_{c_p} = 240 \frac{p}{1013}$$

$$= 0.236p \qquad (D3)$$

where p is the pressure in millibars at the level involved. The amount of carbon dioxide in an elemental slab is then $\Delta u_{c_p} = 0.236\ \Delta p$, values of which are given in column (9). The reduced carbon-dioxide content in an element Δp is $0.236\ \Delta p\sqrt{\frac{p}{p_{SL}}}$, which is given in column (10) of table VII.

Example 1 - cloud indicator at ground level, sighting vertically upward.- Assume that the cloud indicator is sighting on a cloud base at 5600 feet, where the pressure is 825 millibars and the temperature is 11.7° C. For this case only the first four rows of table VII are pertinent. The summations of the reduced quantities of water vapor and carbon dioxide between ground level and each of these levels, and corresponding values of y taken from table V, are given in the following table:

[redacted]

Temperature (°C)	Reduced water vapor above ground level, u_w (cm)	Reduced carbon dioxide above ground level, u_c (cm)	y
21.2	0	0	100
20.9	.48	10	52.4
20.0	.83	18	45.9
9.3	1.97	48	38.4

The values of y are plotted against temperature in the radiation chart and a curve is faired through these points in figure 15. The area under the part of this curve between temperatures of 21.2° C and 11.7° C has been determined by mechanical integration and found to be $277\pi \sin^2\theta$. If the half-angle of the effective field of view is taken to be $2\frac{1}{4}°$, the radiation exchange at the cloud indicator for the specified conditions is 1.34 microwatts per square centimeter of aperture area.

Example 2 - Cloud indicator at altitude, sighting 15° above the horizontal.- Let the cloud indicator be at an altitude of 10,000 feet where the pressure is 699 millibars and the temperature is 3.2° C. Let the line of sight be elevated 15°. Assume further that the instrument is sighting on a cloud at a pressure height of 400 millibars and that the surface temperature of the cloud is the same as the temperature measured by the radiometeorograph at this level, that is, -19.8° C. The last 10 rows of table VII are therefore pertinent for this example.

Equation (26) and figure 10 show that water-vapor and carbon-dioxide contents above the lower surface of the slab - that is, above the cloud indicator - are needed. For this reason, it is necessary to make the summations from a reference level at 699 millibars. A preliminary computation shows that the content of the element between 699 and 662 millibars is 0.197 centimeter of water vapor and 7.1 centimeters of carbon dioxide. In the following table, the summations of these two quantities from the base level of 3.2° C (corresponding to 699 mb) are given in columns (2) and (3):

[redacted]

(1)	(2)	(3)	(4)	(5)	(6)
Temperature (°C)	Reduced amount above 699 mb		Reduced amount along 15° line of sight		y
	Water vapor (cm)	Carbon dioxide (cm)	Water vapor (cm)	Carbon dioxide (cm)	
3.2	0	0	0	0	100
.4	.20	7.1	.76	27	48.1
-4.8	.60	25.3	2.31	98	34.8
-5.6	.64	27.5	2.47	106	34.0
-7.0	.67	29.6	2.58	114	33.6
-8.7	.71	34.4	2.76	133	32.6
-9.6	.72	36.1	2.80	139	32.4
-10.5	.74	40.2	2.88	155	32.0
-13.0	.76	44.2	2.96	171	31.4
-17.8	.79	49.4	3.05	191	32.0
-19.8	.80	51.8	3.08	200	31.9

In order to adapt the table to a line of sight elevated 15°, columns (4) and (5) are included. The values of y are selected from tables III and IV by using the values given here in columns (1), (4), and (5) as the independent parameters.

The values of y are plotted against temperature in figure 15, and the area under the curve is found to be $400\pi \sin^2\theta$. Again, where the half-angle of the effective field of view is taken to be $2\frac{1}{4}^\circ$, the net radiation exchange at the cloud indicator is 1.94 microwatt per square centimeter of aperture area.

[redacted]

REFERENCES

1. Humphreys, W. J.: Physics of the Air. Third ed., McGraw-Hill Book Co., Inc., 1940.

2. Déjardin, Georges: The Light of the Night Sky. Rev. Modern Phys., vol. 8, no. 1, Jan. 1936, pp. 1-21.

3. Pettit, Edison, and Nicholson, Seth B.: Lunar Radiation and Temperatures. Contributions from the Mt. Wilson Observatory, No. 392, Carnegie Inst. of Washington (reprinted from The Astrophysical Jour., vol. LXXI, 1930, pp. 102-135).

4. Becquerel, Jean, and Rossignol, J.: Spectral Absorption of Light and Heat by Pure Inorganic Substances and Miscellaneous Materials (Nonmetals). International Critical Tables, first ed., vol. V. McGraw-Hill Book Co., Inc., 1929.

5. Coblentz, William W.: Investigations of Infra-Red Spectra.
   Part I - Infra-Red Absorption Spectra. Carnegie Inst. of Washington, Pub. No. 35, 1905, pp. 56 and 185.
   Part III - Infra-Red Transmission Spectra. Carnegie Inst. of Washington, Pub. No. 65, 1906, p. 17.

6. Houghton, H. G.: On the Relation between Visibility and the Constitution of Clouds and Fogs. Jour. Aero. Sci., vol. 6, no. 10, Aug. 1939, p. 409.

7. Houghton, Henry G.: The Transmission of Light in the Atmosphere with Applications to Aviation. Jour. Aero. Sci., vol. 9, no. 3, Jan. 1942, p. 104.

8. Wildt, Rupert: The Geochemistry of the Atmosphere and the Constitution of the Terrestrial Planets. Rev. Modern Phys., vol. 14, nos. 2-3, April-July 1942, pp. 151-159.

9. Birge, Raymond T.: A New Table of Values of the General Physical Constants. Rev. Modern Phys., vol. 13, no. 4, Oct. 1941, pp. 233-239.

10. Dobson, G. M. B.: Variations in Atmospheric Ozone and Weather Conditions. Supp. to Quarterly Jour. Roy. Meteorological Soc., vol. 62, 1936, pp 52-54.

[redacted]

11. O'Brien, Brian, Mohler, Fred L., and Stewart, H. S., Jr.: Vertical Distribution of Ozone in the Atmosphere. II - Spectrographic Results of 1935 Flight. The National Geographic Society-U.S. Army Air Corps Stratosphere Flight of 1935 in the Balloon "Explorer II." Nat. Geographic Soc. Contrib. Tech. Papers, Stratosphere Ser., no. 2, 1936, p. 84.

12. Loeb, Leonard B.: The Kinetic Theory of Gases. Second ed., McGraw-Hill Book Co., Inc., 1934, p. 651.

13. Anon.: Smithsonian Meteorological Tables. Fifth rev. ed., Smithsonian Inst., 1939, table 111, p.240.

14. Fowle, F. E.: Water-Vapor Transparency to Low-Temperature Radiation. Smithsonian Misc. Coll., vol. 68, no. 8, 1917, p. 24.

15. Sutherland, G. B. B. M., and Callendar, G. S.: The Infra-Red Spectra of Atmospheric Gases Other Than Water Vapour. Reports on Progress in Physics, vol. IX. The Physical Soc., 1943, pp. 18-28.

16. Callendar, G. S.: Infra-Red Absorption by Carbon Dioxide, with Special Reference to Atmospheric Radiation. Quarterly Jour. Roy. Meteorological Soc., vol. 67, July 1941, pp. 263-274.

17. Adel, Arthur, and Lampland, C. O.: Atmospheric Absorption of Infrared Solar Radiation at the Lowell Observatory.
II. The Spectral Interval: 5.5-8μ. The Astrophysical Jour., vol. 91, no. 1, Jan. 1940, pp. 1-7.
III and IV. The Spectral Intervals: 8.0-11.0μ and 11.0-14.0μ. The Astrophysical Jour., vol. 91, no. 5, June 1940, pp. 481-487.

18. Elsasser, Walter M.: Heat Transfer by Infrared Radiation in the Atmosphere. Harvard Meteorological Studies, No. 6, Harvard Univ., 1942.

[redacted]

19. Strong, John: Study of Atmospheric Absorption and Emission in the Infrared Spectrum. Jour. Franklin Inst., vol. 232, no. 1, July 1941, pp. 1-22.

20. Randall, H. M., Dennison, D. M., Ginsburg, Nathan, and Weber, Louis R.: The Far Infrared Spectrum of Water Vapor. Phys. Rev., vol. 52, no. 3, 2d ser., Aug. 1, 1937, pp. 160-174.

21. Wells, A. J.: The Infra-Red Transmission of Thin Films of Various Organic Materials. Jour. Appl. Phys., vol. 11, no. 2, Feb. 1940, p. 138.

[redacted]

TABLE I

COMPOSITION OF TROPOSPHERE AND APPROXIMATE REDUCED THICKNESS OF SEPARATE CONSTITUENTS IN ENTIRE ATMOSPHERE

[Reduced thickness at 0° C and pressure of 1013 mb; data for first 13 constituents from reference 8; first 2 reduced thicknesses have been corrected by use of Birge's new value for specific volume of an ideal gas (reference 9, p. 234); value for reduced thickness of ozone modified in accordance with ±25-percent variation reported in reference 10, p. 52]

Constituent	Relative volume	Reduced thickness in entire atmosphere
Nitrogen	0.7809	6243.4 m
Oxygen	.2095	1674.9 m
Argon	.0093	74.4 m
Carbon dioxide	.0003	2.4 m
Neon	1.8×10^{-5}	14.4 cm
Helium	5.2×10^{-6}	4.2 cm
Krypton	1×10^{-6}	.8 cm
Hydrogen	5×10^{-7}	.4 cm
Xenon	8×10^{-8}	.06 cm
Ozone	Variable	2 to 4 mm
Nitrogen monoxide	Variable	Several mm
Nitrogen pentoxide	Variable	.03 mm
Total for clean, dry atmosphere		7995.3 m
Water vapor	Very variable	0.5 to 7.0 grams/cm^2
Dust	Variable	3×10^{-6} gram/cm^2

[redacted]

TABLE II

VALUES OF y (EQUATION (31)) FOR TEMPERATURE RANGE FROM -60° C to -38° C

Water-vapor content, u_w (cm) \ Carbon-dioxide content, u_c (cm)	0	0.1	0.25	0.50	1	2	3	5	10	20	30	50	100	200	400	600
0	100	98	96	92	89	86	84	81	79	77	76	74	71	70	69	68
.005	97	95	93	90	87	83	81	78	76	74	73	71	68	67	66	65
.010	96	93	91	88	85	81	79	76	74	72	71	69	67	65	64	63
.025	93	91	88	86	82	78	76	74	72	70	69	67	65	63	62	61
.050	91	89	86	84	80	76	74	72	70	68	67	65	63	61	60	59
.075	90	87	85	83	79	75	73	71	69	67	65	63	62	60	59	58
.100	89	86	84	82	78	74	72	70	68	66	64	62	61	59	58	57
.150	87	84	82	80	76	72	70	68	66	64	62	61	59	58	57	56
.200	85	82	80	78	74	70	68	66	64	62	61	60	58	57	56	55
.250	83	80	78	76	72	69	67	65	63	61	60	59	57	56	55	54
.300	81	79	76	74	71	68	66	64	62	60	59	58	56	55	54	53
.350	79	78	74	72	70	67	65	63	61	59	58	57	55	54	53	52
.400	78	76	73	71	69	66	64	62	60	58	57	56	54	53	52	51
.450	77	75	72	70	68	65	63	61	59	57	56	55	53	52	51	50
.500	76	74	71	69	67	64	62	60	58	56	55	54	52	51	50	49
.600	73	71	69	66	64	61	60	58	56	54	53	52	50	49	48	47
.700	71	69	67	64	62	59	58	56	54	52	51	50	48	47	46	46
.800	69	67	65	62	60	57	56	54	53	51	50	48	47	46	45	45
.900	67	65	63	61	59	56	55	53	52	50	49	47	46	45	44	44
1.000	66	64	62	60	58	55	54	52	51	49	48	46	45	44	43	43
1.200	63	61	59	57	55	53	52	50	49	47	46	44	43	42	41	41
1.400	61	59	57	55	53	51	50	48	47	45	44	42	41	40	39	39
1.600	59	57	55	53	51	49	48	46	45	43	42	41	40	39	38	38
1.800	57	55	53	51	49	47	46	45	43	42	41	40	39	38	37	37
2.000	55	54	52	50	48	46	45	44	42	41	40	39	38	37	36	36

TABLE II - Concluded

VALUES OF y - Concluded

Water-vapor content, u_w (cm) \ Carbon-dioxide content, u_c (cm)	0	0.1	0.25	0.50	1	2	3	5	10	20	30	50	100	200	400	600
2.500	51	50	49	47	45	44	42	41	40	39	38	37	36	35	34	34
3.000	48	47	46	44	43	41	40	39	38	37	36	35	34	33	32	32
3.500	46	45	43	42	41	39	38	37	36	35	34	33	32	31	30	30
4.000	44	43	41	40	39	37	36	35	34	33	32	31	30	30	29	29
4.500	42	41	39	38	37	35	34	33	32	31	31	30	29	29	28	28
5.000	40	39	38	37	35	33	33	32	31	30	30	29	28	28	27	27
6.000	37	36	35	34	32	31	30	30	29	28	27	27	26	26	25	25
7.000	34	33	32	31	30	29	28	28	27	26	25	25	24	24	23	23
8.000	31	30	30	29	28	27	26	26	25	24	23	23	22	22	21	21
9.000	29	28	28	27	26	25	24	24	23	22	22	21	21	21	20	20
10.000	27	26	26	25	24	24	23	23	22	21	21	20	20	20	19	19
12.000	24	23	23	22	21	21	20	20	20	19	19	18	18	18	17	17
14.000	21	20	20	20	19	18	18	18	18	17	17	16	16	16	15	15
16.000	19	18	18	18	17	16	16	16	16	15	15	14	14	14	13	13
18.000	17	16	16	16	15	14	14	14	14	13	13	12	12	12	12	12
20.000	15	14	14	14	13	12	12	12	12	11	11	11	11	11	11	11
22.000	13	12	12	12	11	11	11	10	10	10	10	10	10	10	10	10
24.000	11	11	10	10	10	10	10	9	9	9	9	9	9	9	9	9
26.000	10	10	9	9	9	9	9	8	8	8	8	8	8	8	8	8

NATIONAL ADVISORY
COMMITTEE FOR AERONAUTICS

TABLE III

VALUES OF y (EQUATION (31)) FOR TEMPERATURE RANGE FROM -38° C to -17° C

Water-vapor content, u_w (cm) \ Carbon-dioxide content, u_c (cm)	0	0.1	0.25	0.50	1	2	3	5	10	20	30	50	100	200	400	600
0	100	98	96	93	90	87	86	83	81	79	78	76	74	73	72	71
.005	96	94	92	89	86	83	82	79	77	75	74	72	70	69	68	67
.010	94	92	89	87	84	81	79	76	75	73	72	70	68	67	66	65
.025	91	89	86	84	81	78	76	74	72	70	68	67	65	64	63	62
.050	88	86	84	81	78	75	73	71	69	67	66	64	63	61	60	60
.075	86	85	82	79	77	73	71	70	67	66	64	63	61	60	59	58
.100	85	84	81	78	76	72	70	69	66	65	63	62	60	59	58	57
.150	83	82	79	76	74	70	68	67	64	63	61	60	58	57	56	56
.200	81	80	77	74	72	68	66	65	63	61	60	59	57	56	55	55
.250	79	78	75	72	70	67	65	64	62	60	59	58	56	55	54	54
.300	77	76	73	71	68	66	64	63	61	59	58	57	55	54	53	53
.350	76	74	72	70	67	64	63	62	60	58	57	56	54	53	52	52
.400	75	73	71	69	66	63	62	61	59	57	56	55	53	52	51	51
.450	74	72	70	68	65	62	61	60	58	56	55	54	52	51	50	50
.500	73	71	69	67	64	61	60	59	57	55	54	53	51	50	49	49
.600	70	68	66	64	62	59	58	56	55	53	52	51	49	48	47	47
.700	68	66	64	62	60	57	56	54	53	51	50	49	47	47	46	45
.800	66	64	62	60	58	56	54	53	51	50	49	48	46	46	45	44
.900	64	62	60	58	57	55	53	52	50	49	48	47	45	45	44	43
1.000	63	61	59	57	56	54	52	51	49	48	47	46	44	44	43	42
1.200	60	59	57	55	53	51	50	49	47	46	45	44	42	42	41	40
1.400	58	57	55	53	51	49	48	47	45	44	43	42	40	40	39	38
1.600	56	55	53	51	49	47	46	45	43	42	41	40	39	39	38	37
1.800	54	53	51	50	48	46	45	44	42	41	40	39	38	38	37	36
2.000	53	51	50	49	47	45	44	43	41	40	39	38	37	37	36	35

TABLE III - Concluded

VALUES OF y - Concluded

Water-vapor content, u_w (cm) \ Carbon-dioxide content, u_c (cm)	0	0.1	0.25	0.50	1	2	3	5	10	20	30	50	100	200	400	600
2.500	49	48	46	46	44	42	41	40	38	38	37	36	35	34	34	33
3.000	46	45	43	43	41	40	39	38	36	36	35	34	33	32	32	31
3.500	44	43	41	40	39	38	37	36	34	34	33	32	31	30	30	29
4.000	42	41	39	38	37	36	35	34	33	32	31	31	30	29	28	28
4.500	40	39	37	36	35	34	33	32	32	31	30	30	29	28	27	27
5.000	38	37	36	35	34	33	32	31	31	30	29	29	28	27	26	26
6.000	35	34	33	32	31	30	29	29	28	27	26	26	25	25	24	24
7.000	32	31	31	30	29	28	27	27	26	25	24	24	23	23	22	22
8.000	30	29	29	28	27	26	25	25	24	23	22	22	21	21	21	21
9.000	28	27	27	26	25	24	23	23	22	22	21	21	20	20	20	20
10.000	26	26	25	24	23	23	22	22	21	21	20	20	19	19	19	19
12.000	23	23	22	21	20	20	20	19	19	19	18	18	17	17	17	17
14.000	21	20	20	19	18	18	18	17	17	17	16	16	15	15	15	15
16.000	19	18	18	17	16	16	16	15	15	15	14	14	13	13	13	13
18.000	17	16	16	15	14	14	14	13	13	13	12	12	12	12	11	11
20.000	15	14	14	13	12	12	12	12	11	11	11	11	11	11	10	10
22.000	13	12	12	11	11	10	10	10	10	10	10	10	10	10	9	9
24.000	11	11	10	10	10	9	9	9	9	9	9	9	9	9	8	8
26.000	10	10	9	9	9	8	8	8	8	8	8	8	8	8	7	7

TABLE IV

VALUES OF y (EQUATION (31)) FOR TEMPERATURE RANGE FROM -17° C to 9° C

Water-vapor content, u_w (cm) \ Carbon-dioxide content, u_c (cm)	0	0.1	0.25	0.50	1	2	3	5	10	20	30	50	100	200	400	600
0	100	98	96	93	91	89	87	86	83	82	80	79	77	76	75	74
.005	95	93	91	88	86	83	82	80	78	76	75	74	72	71	70	69
.010	92	90	87	85	82	80	79	77	75	73	72	71	69	68	67	66
.025	88	86	84	81	79	76	74	73	71	69	68	67	65	64	63	63
.050	85	83	81	78	76	73	71	70	68	66	65	64	62	61	60	60
.075	83	81	79	76	74	72	70	68	66	64	63	62	60	59	58	58
.100	82	80	78	75	73	70	68	66	65	63	62	61	59	58	57	57
.150	80	78	75	73	71	68	66	64	63	61	60	59	58	57	56	55
.200	78	76	73	71	69	66	65	63	62	60	59	58	56	55	54	54
.250	76	74	72	70	68	65	63	62	60	59	58	56	55	54	53	53
.300	74	72	70	68	66	64	62	61	59	57	56	55	54	53	52	52
.350	73	71	69	67	65	63	61	59	58	56	55	54	52	51	51	51
.400	72	70	67	65	63	61	60	58	56	55	54	53	51	50	50	50
.450	70	68	66	64	62	60	59	57	55	54	53	52	51	50	49	49
.500	67	67	65	63	61	59	58	56	54	53	52	51	50	49	48	48
.600	66	65	63	61	59	57	56	54	53	51	50	49	48	47	46	46
.700	65	63	61	59	57	55	54	52	51	50	49	48	47	46	45	45
.800	63	61	59	57	56	54	52	51	50	48	47	46	45	44	44	43
.900	62	60	58	56	54	52	51	50	48	47	46	45	44	43	43	42
1.000	60	58	56	55	53	51	50	48	47	46	45	44	43	42	42	41
1.200	57	56	54	53	51	49	48	46	45	44	43	42	41	41	40	40
1.400	55	54	52	51	49	47	46	45	44	42	42	41	40	39	38	38
1.600	53	52	51	49	47	45	44	43	42	41	40	40	39	38	37	37
1.800	52	51	49	48	46	44	43	42	41	40	39	38	37	36	36	35
2.000	50	49	47	46	44	43	42	41	40	39	38	37	36	35	35	34

TABLE IV - Concluded

VALUES OF y - Concluded

Water-vapor content, u_w (cm) \ Carbon-dioxide content, u_c (cm)	0	0.1	0.25	0.50	1	2	3	5	10	20	30	50	100	200	400	600
2.500	47	46	44	43	42	40	39	38	37	36	35	34	34	33	33	32
3.000	44	43	42	41	40	38	37	36	35	34	34	33	32	31	31	30
3.500	42	41	40	39	38	36	35	34	33	32	32	31	30	30	29	29
4.000	40	39	38	37	36	35	34	33	32	31	31	30	29	28	28	27
4.500	38	37	36	35	34	33	32	31	30	30	29	28	28	27	27	26
5.000	37	36	34	33	32	31	30	30	29	28	28	27	26	26	26	25
6.000	34	33	32	31	30	29	28	28	27	26	26	25	24	24	24	23
7.000	31	30	29	28	28	27	26	26	25	24	24	23	23	22	22	22
8.000	29	28	27	26	26	25	24	24	23	22	22	22	21	21	21	20
9.000	27	26	25	25	24	23	23	22	22	21	21	20	20	20	19	19
10.000	26	24	24	23	23	22	21	21	20	20	20	19	19	18	18	18
12.000	23	22	21	20	20	19	19	18	18	18	18	17	17	16	16	16
14.000	20	20	19	18	18	17	17	16	16	16	16	15	15	15	15	14
16.000	18	18	17	16	16	15	15	15	14	14	14	14	14	13	13	13
18.000	16	16	15	15	14	14	14	13	13	13	13	12	12	12	12	12
20.000	15	14	14	13	13	12	12	12	12	12	11	11	11	11	11	11
22.000	13	12	12	12	12	11	11	10	10	10	10	10	10	10	10	9
24.000	12	11	11	10	10	10	10	9	9	9	9	9	9	9	8	8
26.000	10	10	9	9	8	8	8	8	8	8	8	8	7	7	7	7

TABLE V

VALUES OF y (EQUATION (31)) FOR TEMPERATURE RANGE FROM 9° C TO 26° C

Water-vapor content, u_w (cm) \ Carbon-dioxide content, u_c (cm)	0	0.1	0.25	0.50	1	2	3	5	10	20	30	50	100	200	400	600
0	100	98	96	94	91	89	88	87	84	83	82	81	80	78	78	77
.005	94	92	90	88	85	83	82	80	78	77	76	75	74	72	72	71
.010	90	88	86	84	82	79	78	76	74	73	72	71	70	68	68	67
.025	86	84	81	79	77	74	73	72	70	68	68	66	65	64	63	63
.050	82	80	78	76	74	71	70	68	66	65	64	63	62	60	60	59
.075	80	78	76	74	72	69	68	66	64	63	62	61	60	58	58	57
.100	78	77	74	72	70	68	66	64	63	62	60	59	58	57	56	56
.150	76	74	72	70	68	66	64	62	60	60	58	57	56	55	54	54
.200	74	72	70	68	66	64	62	60	58	58	56	55	54	53	52	52
.250	72	70	68	66	64	62	60	58	57	56	55	54	53	52	51	51
.300	71	68	66	64	62	60	59	57	56	55	54	53	52	51	50	50
.350	69	67	64	63	61	59	58	56	55	54	53	52	51	50	49	49
.400	68	66	63	62	60	58	57	55	54	53	52	51	50	49	48	48
.450	67	65	62	61	59	57	56	54	53	52	51	50	49	48	47	47
.500	66	64	61	60	58	56	55	53	52	51	50	49	48	47	46	46
.600	63	61	59	58	56	54	53	51	50	49	48	47	46	45	44	44
.700	61	59	57	56	54	52	51	49	48	47	46	46	45	44	43	43
.800	59	57	56	54	52	51	50	48	47	46	45	45	44	43	42	42
.900	58	56	55	53	51	50	49	47	46	45	44	44	43	42	41	41
1.000	57	55	54	52	50	49	48	46	45	44	43	43	42	41	40	40
1.200	54	53	51	50	48	46	45	44	43	42	41	41	40	39	38	38
1.400	52	51	49	48	46	44	43	42	41	40	39	39	38	37	37	36
1.600	50	49	47	46	44	43	42	41	40	39	38	37	37	36	36	35
1.800	49	48	46	45	43	42	41	40	39	38	37	36	36	35	35	34
2.000	48	47	45	44	42	41	40	39	38	37	36	35	35	34	34	33

TABLE V - Concluded

VALUES OF y - Concluded

Water-vapor content, u_w (cm) \ Carbon-dioxide content, u_c (cm)	0	0.1	0.25	0.50	1	2	3	5	10	20	30	50	100	200	400	600
2.500	45	44	42	41	39	38	37	36	35	34	34	33	32	32	32	31
3.000	42	41	40	39	37	36	35	34	33	32	32	31	30	30	30	29
3.500	40	39	38	37	35	34	33	32	31	30	30	29	29	28	28	27
4.000	38	37	36	35	33	32	31	30	29	29	29	28	28	27	27	26
4.500	36	35	34	33	32	31	30	29	28	28	28	27	27	26	26	25
5.000	35	34	33	32	31	30	29	28	27	27	27	26	26	25	25	24
6.000	32	31	30	29	28	27	26	26	25	25	25	24	24	23	23	22
7.000	30	29	28	27	26	25	24	24	23	23	23	22	22	21	21	20
8.000	28	27	26	25	24	23	23	22	21	21	21	20	20	20	19	19
9.000	26	25	24	23	22	22	22	21	20	20	20	19	19	19	18	18
10.000	25	24	22	22	21	21	21	20	19	19	19	18	18	18	17	17
12.000	22	21	20	20	19	18	18	18	17	17	17	16	16	16	15	15
14.000	20	19	18	18	17	16	16	16	15	15	15	14	14	14	13	13
16.000	18	17	16	16	15	14	14	14	13	13	13	13	13	13	12	12
18.000	16	15	14	14	13	12	12	12	12	12	12	12	12	12	11	11
20.000	14	13	12	12	12	11	11	11	11	11	11	11	11	11	10	10
22.000	13	12	11	11	11	10	10	10	10	10	10	10	10	10	9	9
24.000	12	11	10	10	10	9	9	9	9	9	9	9	9	9	8	8
26.000	11	10	9	9	9	8	8	8	8	8	8	8	8	8	7	7

TABLE VI

VALUES OF y (EQUATION (31)) FOR TEMPERATURE RANGE FROM 26° C TO 50° C

Water-vapor content, u_w (cm) \ Carbon-dioxide content, u_c (cm)	0	0.1	0.25	0.50	1	2	3	5	10	20	30	50	100	200	400	600
0	100	98	96	94	92	90	88	87	86	84	83	82	81	80	80	79
.005	93	91	89	87	85	83	81	80	79	77	76	75	74	73	73	72
.010	88	86	84	82	80	78	77	75	74	73	72	71	70	68	68	68
.025	83	81	79	77	75	73	72	70	69	68	67	66	64	63	63	62
.050	79	77	75	73	71	69	68	66	65	64	63	62	60	59	59	58
.075	77	75	73	71	69	67	66	64	63	62	60	59	58	57	56	56
.100	75	73	71	69	67	65	64	62	61	60	58	57	56	56	55	54
.150	72	70	68	66	64	63	61	60	58	57	56	55	54	53	52	52
.200	70	68	66	64	62	61	59	58	56	55	54	53	52	51	50	50
.250	68	66	64	62	60	59	57	56	54	53	53	52	51	50	49	49
.300	66	64	62	61	59	57	56	55	53	52	52	51	50	49	48	48
.350	65	63	61	60	58	56	55	54	52	51	51	50	49	48	47	47
.400	64	62	60	59	57	55	54	53	51	50	50	49	48	47	46	46
.450	63	61	59	58	56	54	53	52	50	49	49	48	47	46	45	45
.500	62	60	58	57	55	53	52	51	49	48	48	47	46	45	44	44
.600	60	58	56	54	53	51	50	49	47	46	46	45	44	43	42	42
.700	58	56	54	52	51	49	48	47	46	45	44	44	43	42	41	41
.800	56	54	52	51	49	48	47	46	45	44	43	43	42	41	40	40
.900	55	53	51	50	48	47	46	45	44	43	42	42	41	40	39	39
1.000	54	52	50	49	47	46	45	44	43	42	41	41	40	39	38	38
1.200	52	50	48	47	45	44	43	42	41	40	39	38	38	37	36	36
1.400	50	48	46	45	43	42	41	40	39	38	37	37	36	35	35	34
1.600	48	46	44	43	42	40	39	38	38	37	36	36	35	34	34	33
1.800	46	45	43	42	41	39	38	37	37	36	35	35	34	33	33	32
2.000	45	44	42	41	40	38	37	36	36	35	34	34	33	32	32	31

TABLE VI - Concluded

VALUES OF y - Concluded

Water-vapor content, u_w (cm) \ Carbon-dioxide content, u_c (cm)	0	0.1	0.25	0.50	1	2	3	5	10	20	30	50	100	200	400	600
2.500	42	41	39	38	37	36	35	34	33	33	32	32	31	30	30	29
3.000	40	39	37	36	35	34	33	32	31	31	30	30	29	28	28	27
3.500	38	37	35	34	33	32	31	30	29	29	28	28	27	27	26	26
4.000	36	35	33	32	31	30	29	29	28	27	27	27	26	26	25	25
4.500	35	33	32	31	30	29	28	28	27	26	26	26	25	25	24	24
5.000	34	32	31	30	29	28	27	27	26	25	25	25	24	24	23	23
6.000	31	30	29	28	27	26	25	25	24	23	23	23	22	22	21	21
7.000	29	28	27	26	25	24	23	23	22	21	21	21	20	20	19	19
8.000	27	26	25	24	23	22	21	21	20	20	20	19	19	19	18	18
9.000	25	24	23	22	21	20	20	20	19	19	19	18	18	18	17	17
10.000	24	23	22	21	20	19	19	19	18	18	18	17	17	17	16	16
12.000	22	20	20	19	18	18	18	17	17	16	16	15	15	15	15	15
14.000	20	18	18	17	16	16	16	15	15	14	14	13	13	13	13	13
16.000	18	16	16	15	14	14	14	13	13	12	12	12	12	12	12	12
18.000	16	14	14	13	12	12	12	12	12	11	11	11	11	11	11	11
20.000	14	13	13	12	11	11	11	11	11	10	10	10	10	10	10	10
22.000	13	12	12	11	10	10	10	10	10	9	9	9	9	9	9	9
24.000	12	11	11	10	9	9	9	9	9	8	8	8	8	8	8	8
26.000	11	10	10	9	8	8	8	8	8	7	7	7	7	7	7	7

[redacted]

TABLE VII

RESULTS BASED ON PRELIMINARY SAMPLE COMPUTATIONS FOR APPENDIX D

[Data in columns (1) to (3) from radiometeorograph ascent of October 1, 1943 from Langley Field, Va.]

(1) Pressure, p (mb)	(2) Temperature ($^{\circ}$C)	(3) Relative humidity, h	(4) Specific humidity, q	(5) $q\sqrt{\frac{p}{p_{SL}}}$	(6) Mean of (5)	(7) Δp (mb)	(8) $\frac{(6) \times (7)}{0.980}$ (cm)	(9) 0.236 Δp	(10) (9) $\times \sqrt{\frac{p}{p_{SL}}}$ mean (cm)
1014	21.2	0.78	12.2×10^{-3}	12.2×10^{-3}					
					11.3×10^{-3}	42	484×10^{-3}	9.91	9.8
972	20.9	.66	10.6	10.4					
					9.59	35	342	8.26	8.0
937	20.0	.58	9.14	8.79					
					7.95	141	1143	33.3	30.7
796	9.3	.88	8.04	7.12					
					5.93	134	811	31.6	26.8
662	.4	1.00	5.86	4.74					
					3.97	99	401	23.4	18.2
563	-4.8	.90	4.30	3.20					
					3.07	13	41	3.07	2.2
550	-5.6	.87	3.98	2.93					
					2.36	12	29	2.83	2.1
538	-7.0	.58	2.44	1.78					
					1.58	28	45	6.61	4.8
510	-8.7	.50	1.95	1.38					
					1.04	10	11	2.36	1.7
500	-9.6	.27	1.00	.70					
					.78	25	20	5.90	4.1
475	-10.5	.35	1.26	.86					
					.83	25	21	5.90	4.0
450	-13.0	.39	1.21	.80					
					.68	34	24	8.02	5.2
416	-17.8	.38	.86	.55					
					.49	16	8	3.78	2.4
400	-19.8	.33	.66	.42					

[redacted]

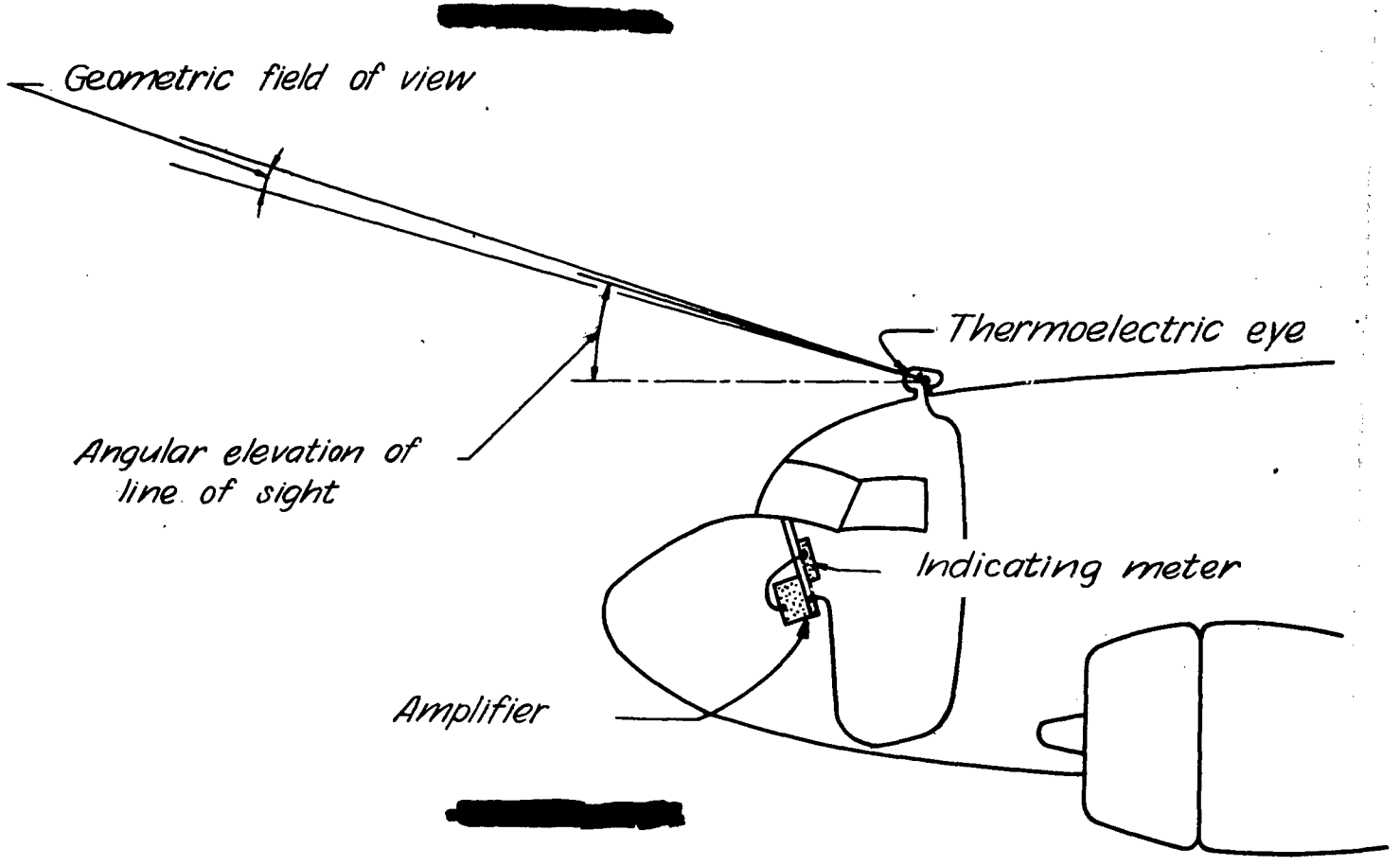

NATIONAL ADVISORY COMMITTEE FOR AERONAUTICS

Figure 1.- Cloud indicator installed in airplane.

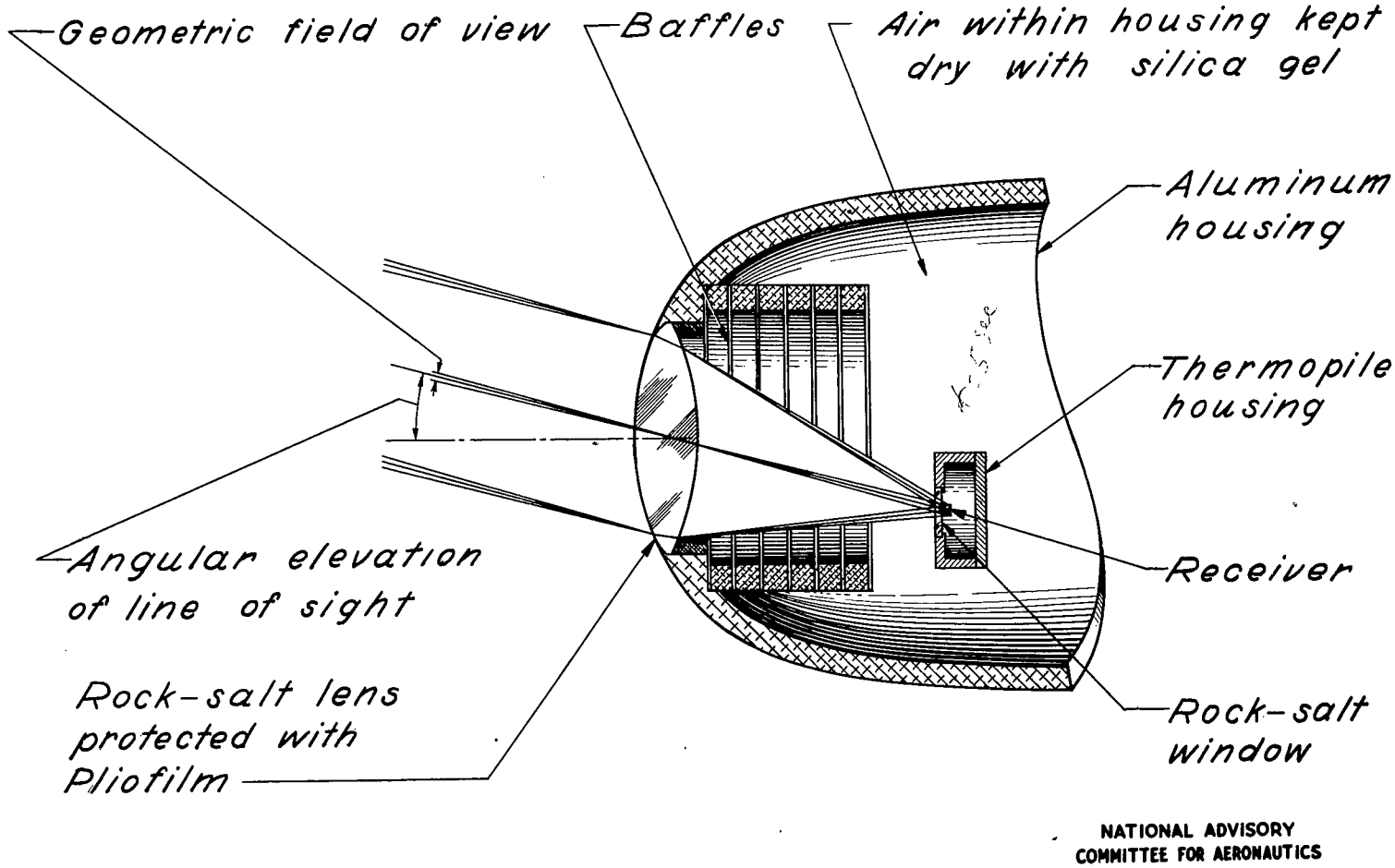

Figure 2.- Optical system of thermoelectric eye.

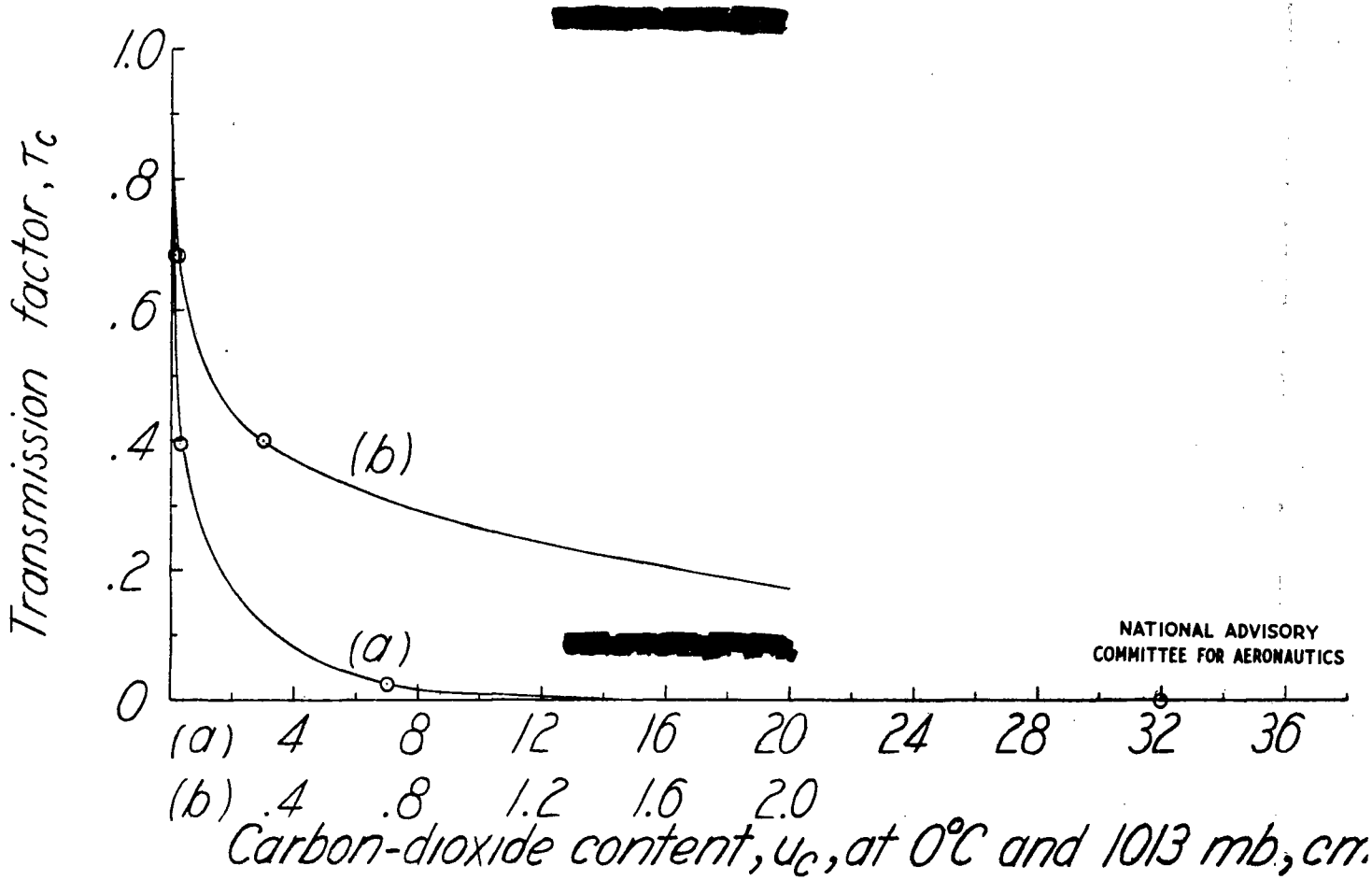

Figure 3.-Average transmission of carbon dioxide from 2220 to 2500 cm^{-1}. $\tau_c = \frac{10}{9}(\tau_c' - 0.1)$; τ_c' from reference 14. (See also reference 15.)

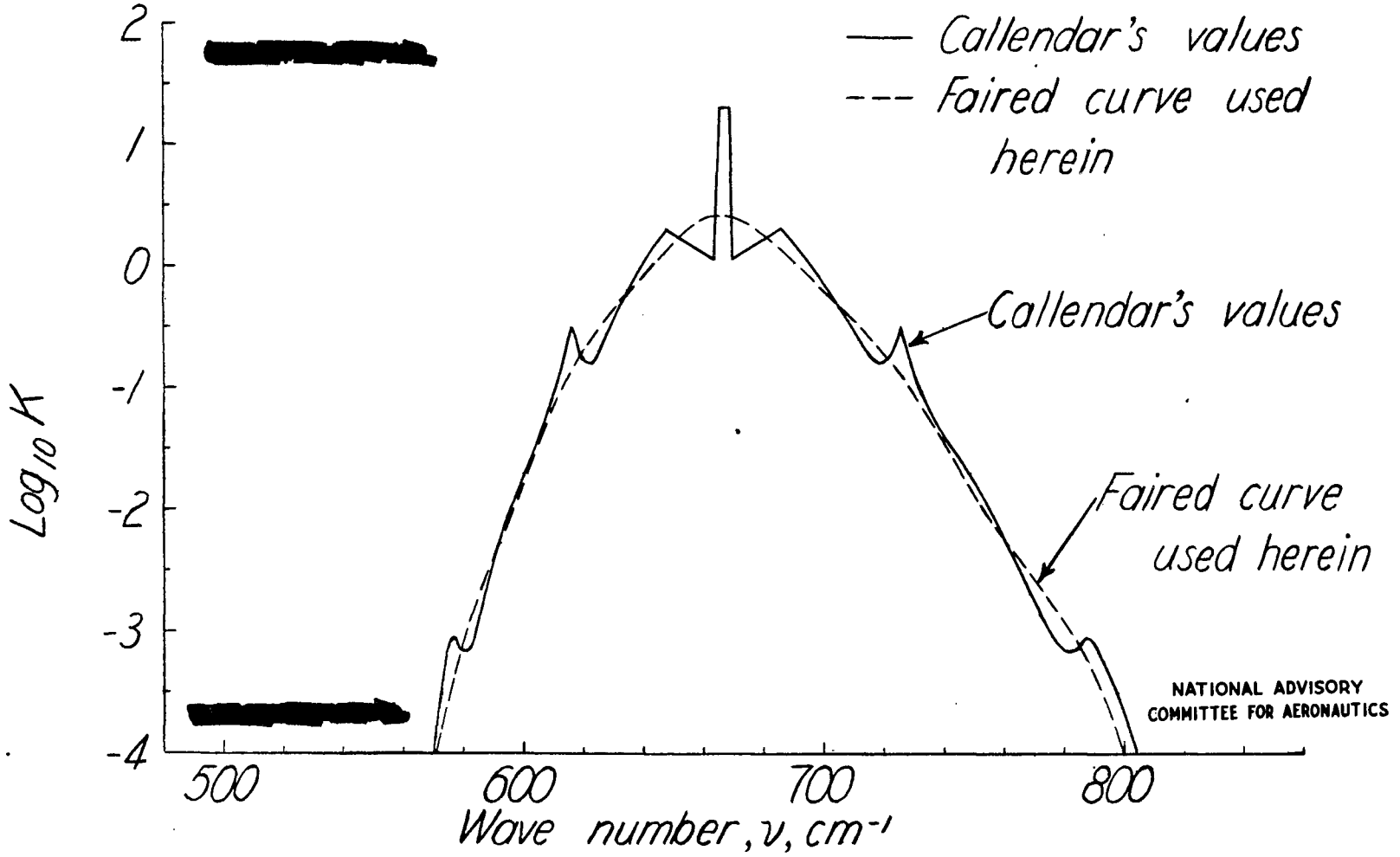

Figure 4.-Callendar's spectral-absorption coefficient K for the 667 cm^{-1} band of carbon dioxide (reference 16).

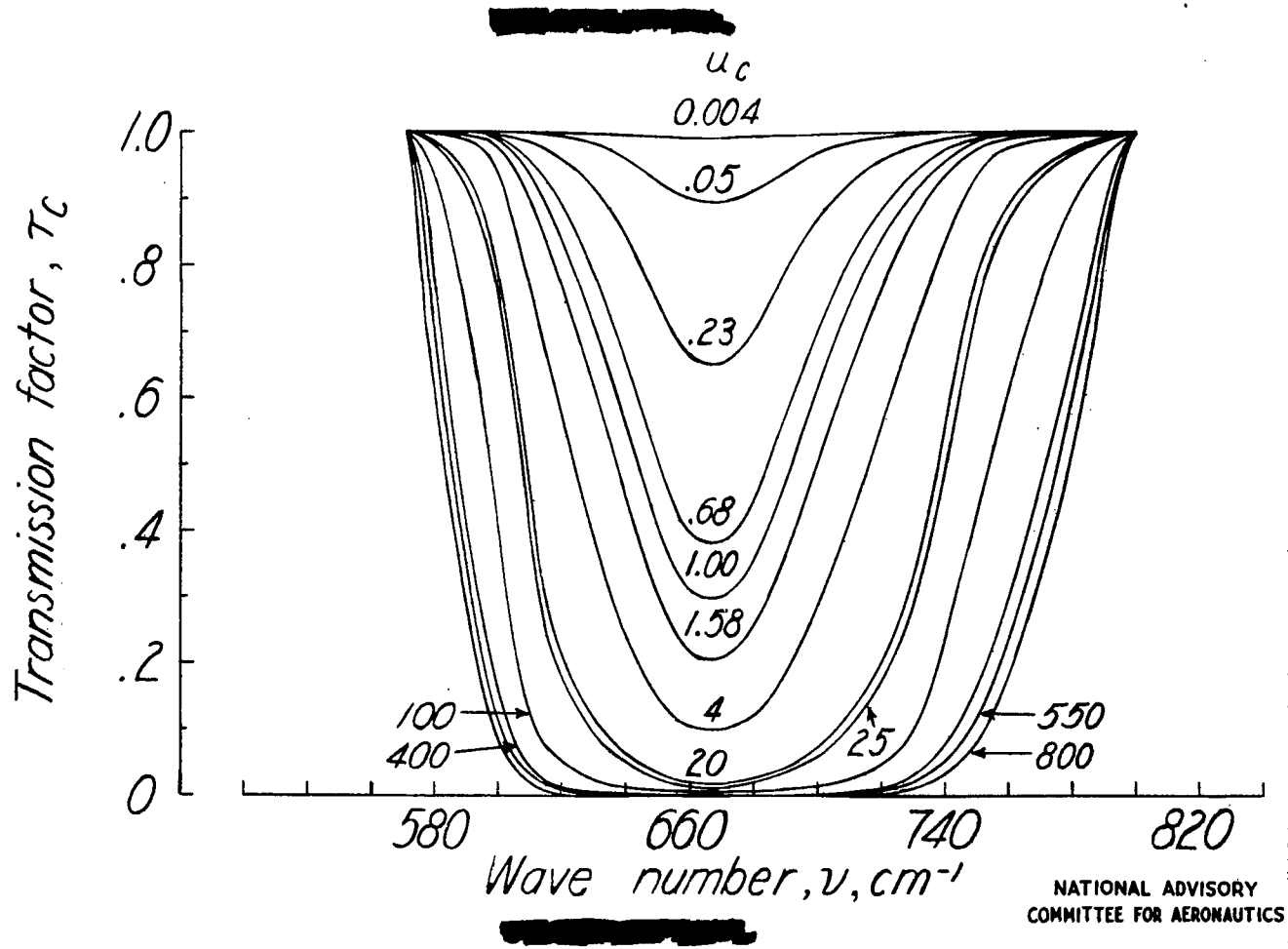

Figure 5.- Spectral transmission factor for the 667 cm^{-1} band of carbon dioxide. u_c, carbon-dioxide content, in centimeters, at 0° C and 1013 millibars.

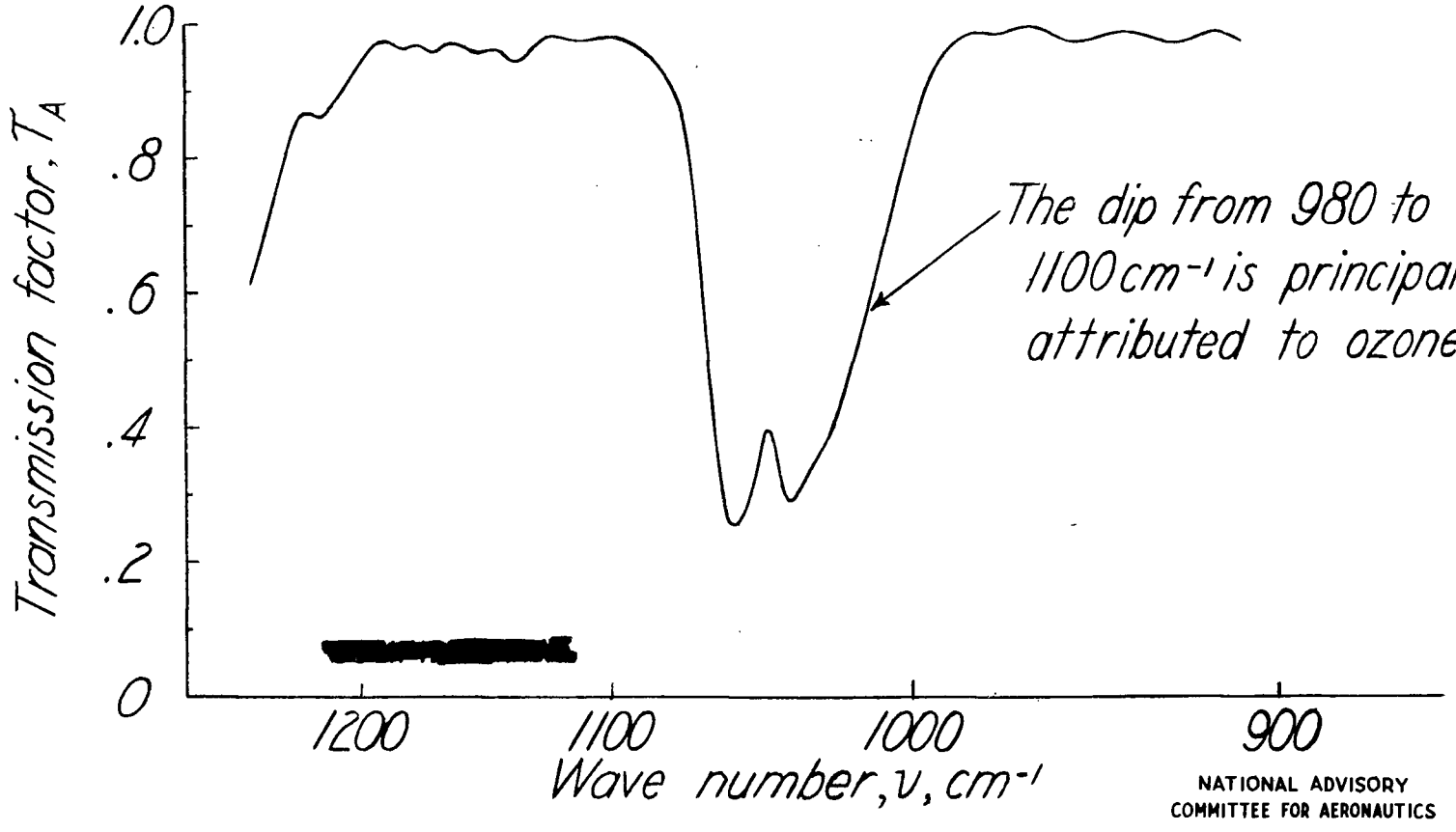

Figure 6.-Spectral transmission factor of the atmosphere for solar radiation. Water-vapor content, 0.21 centimeter of precipitable water vapor; air mass, 1.5 (reference 17).

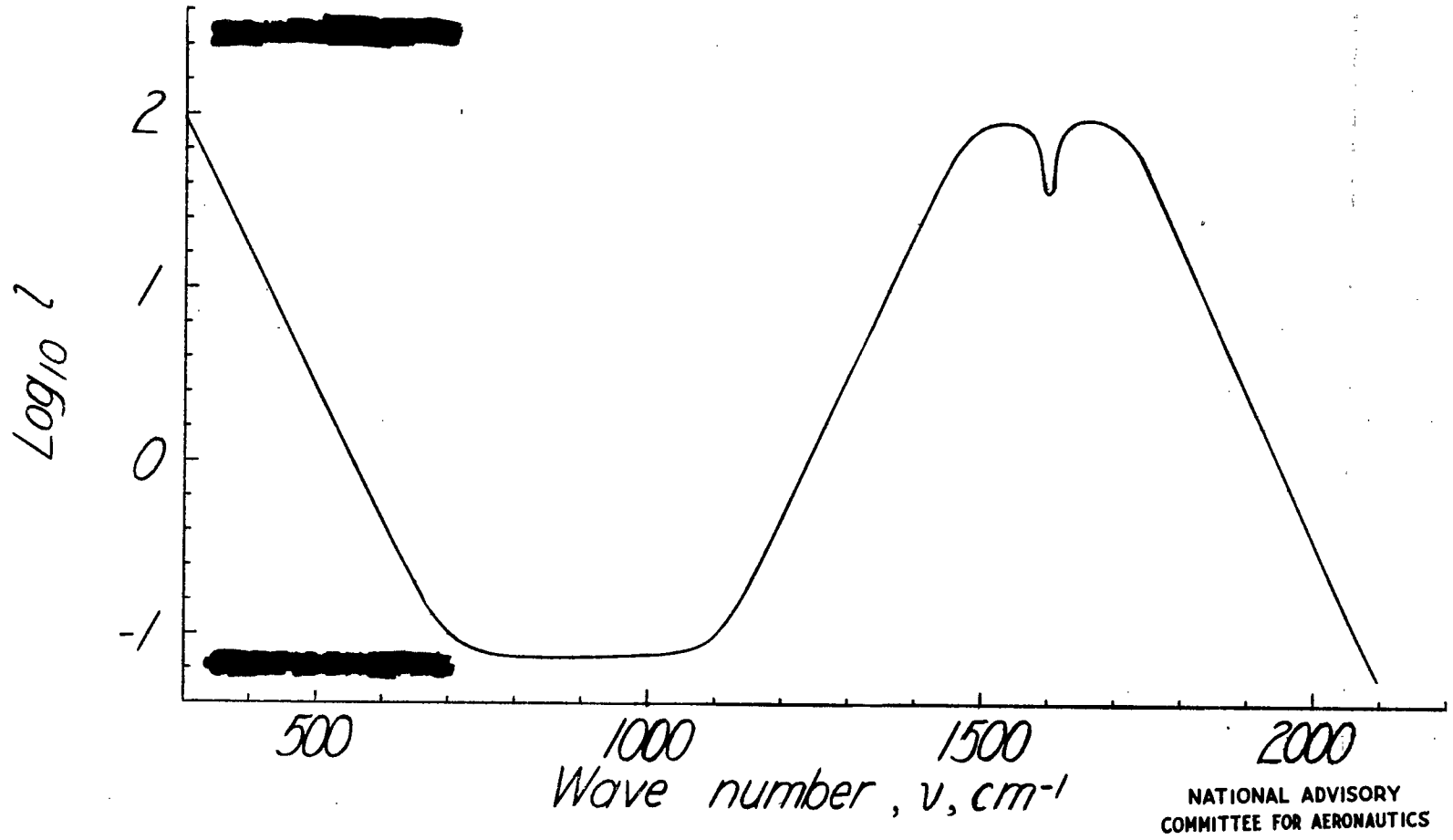

Figure 7.-Generalized absorption coefficient l for water vapor. (From fig. 19, p. 57, reference 18).

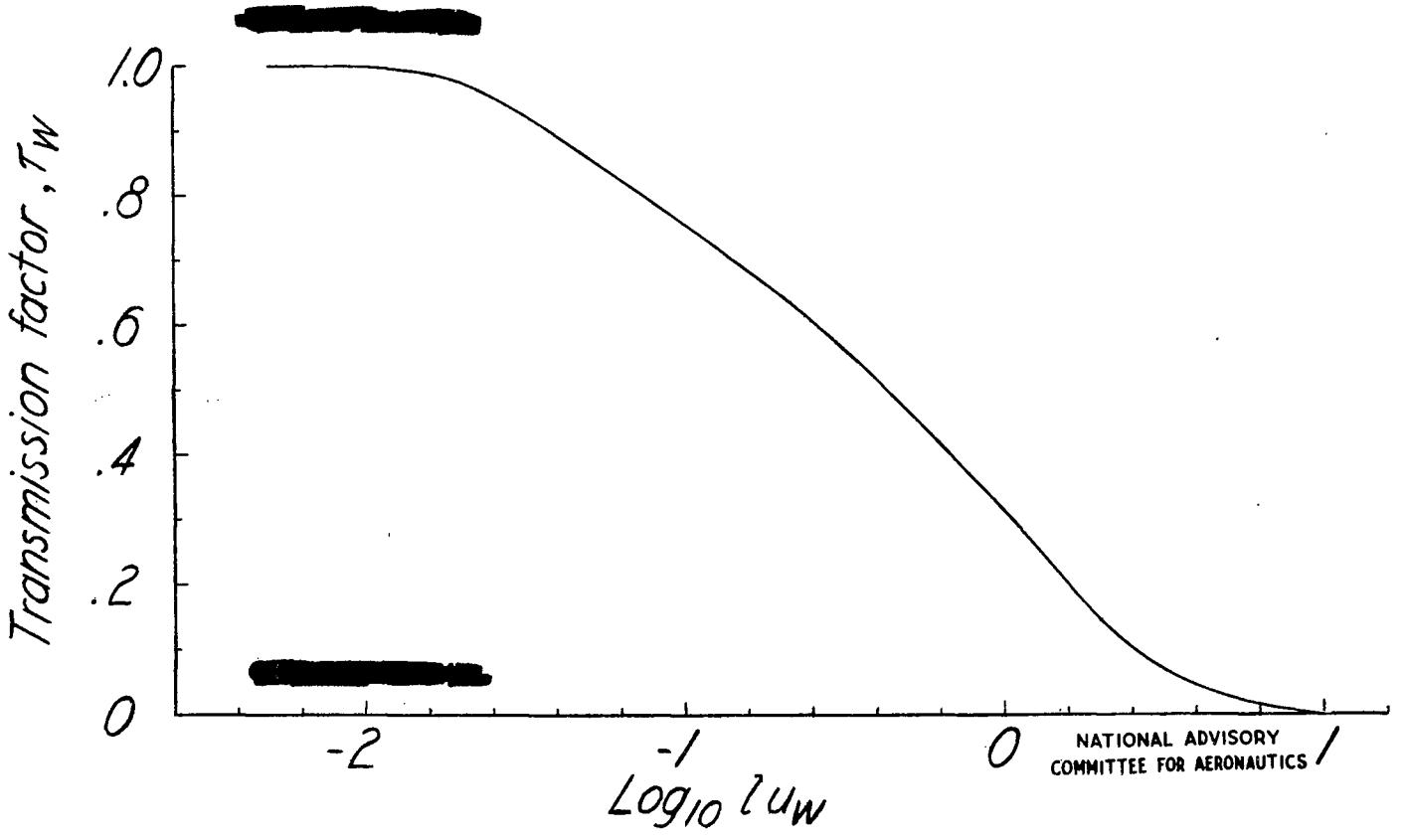

Figure 8.-Transmission factor for parallel-beam radiation as a function of $l u_w$. (From fig. 15, p. 43 of reference 18). l, Elsasser's generalized absorption coefficient; u_w, number of centimeters of precipitable water vapor.

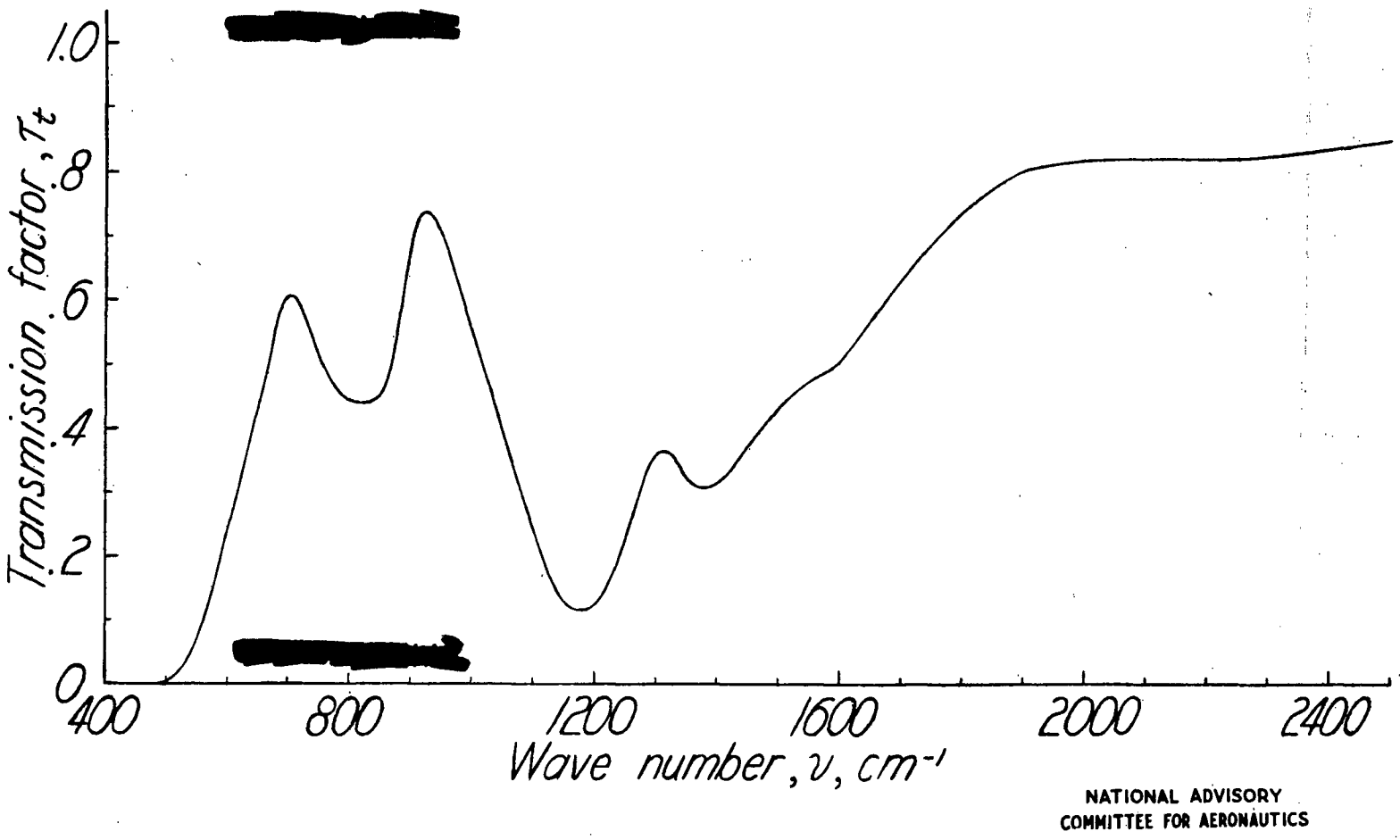

Figure 9.-Spectral transmission of optical path within thermoelectric eye.

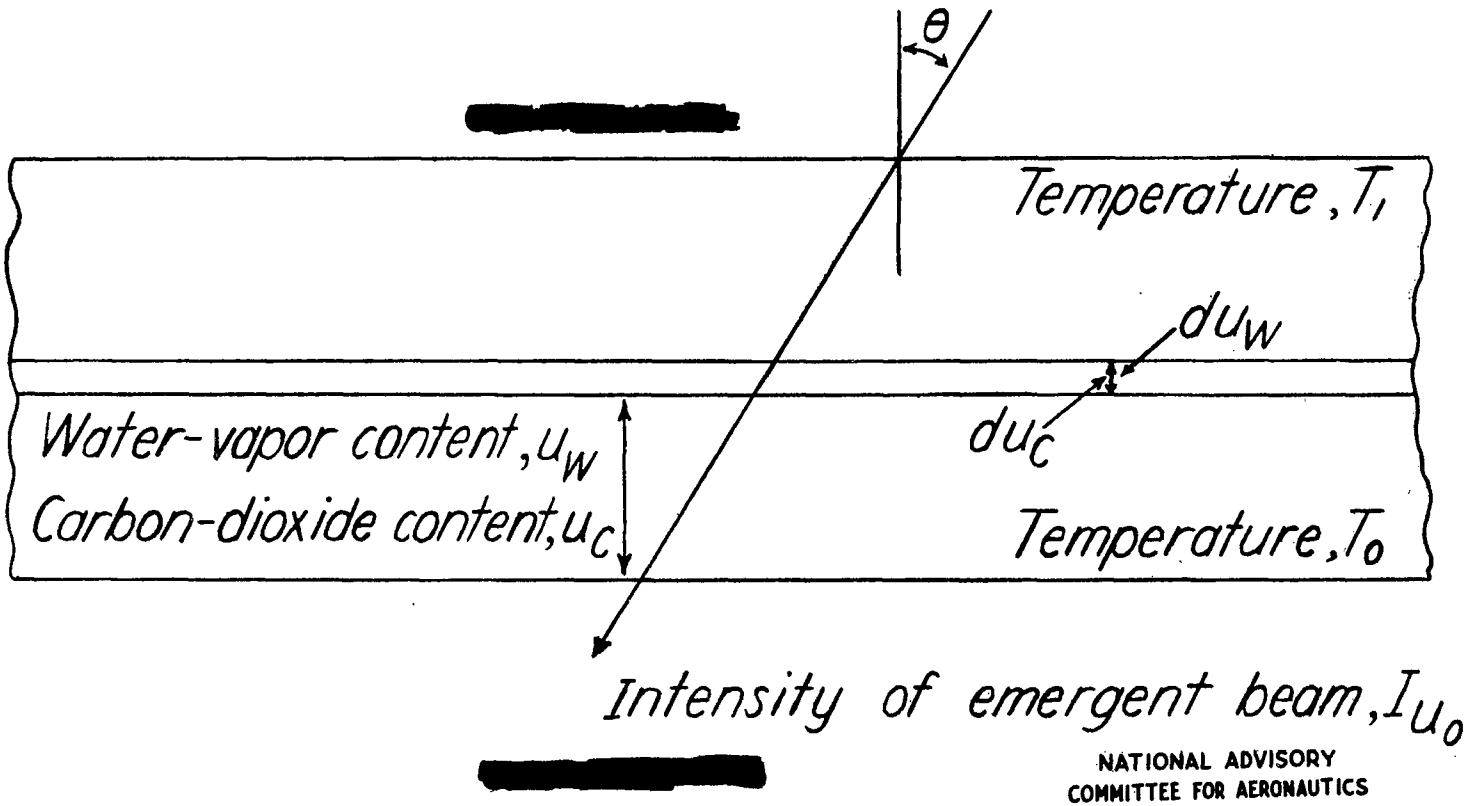

Figure 10.-Horizontal slab of atmosphere, homogeneous in any horizontal plane, as used in derivation of equation (10).

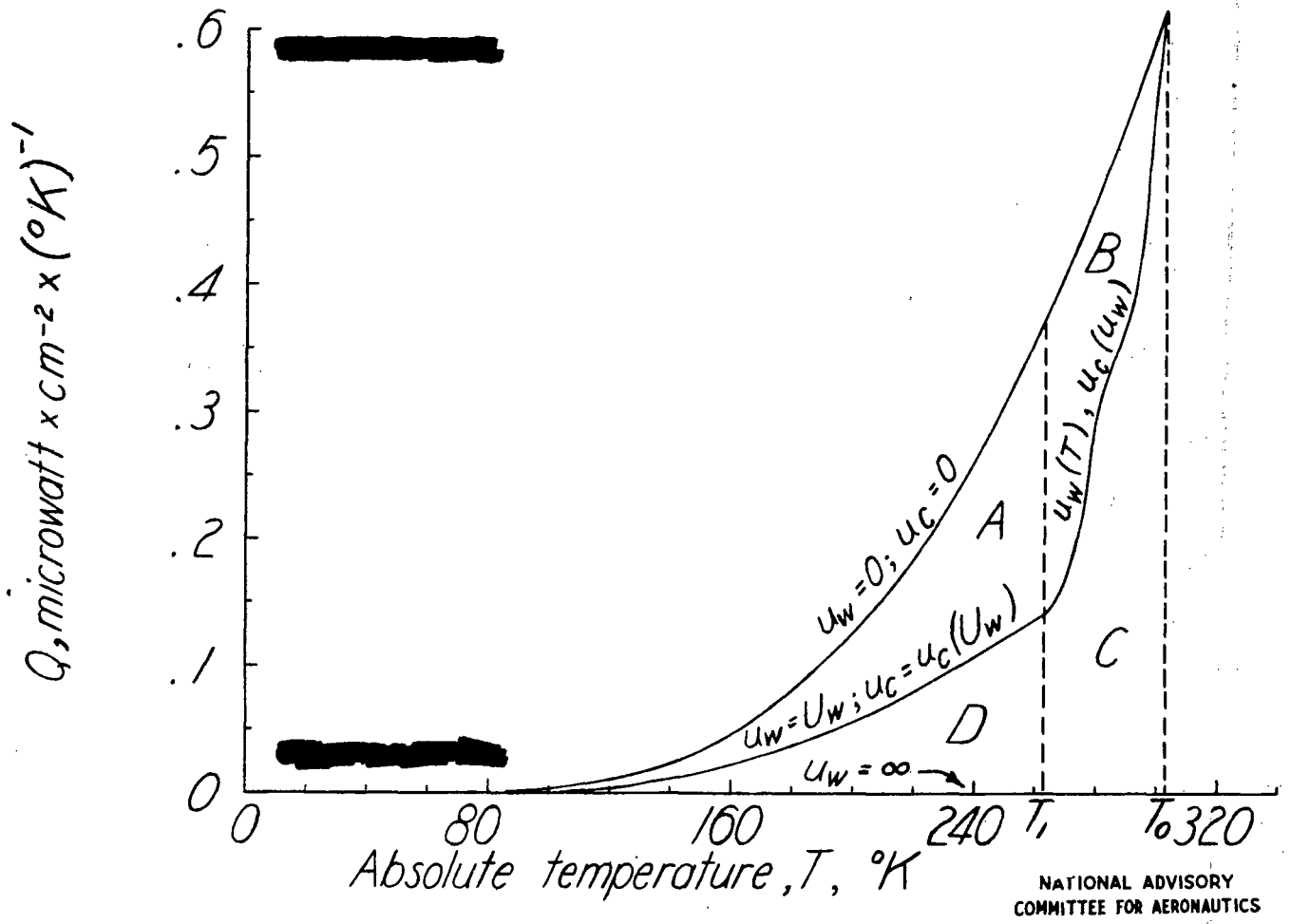

Figure 11.- Closed curve on a QT-plane, representing a certain atmosphere in which the carbon-dioxide content u_c is a function of the water-vapor content u_w. (See equation (26).)

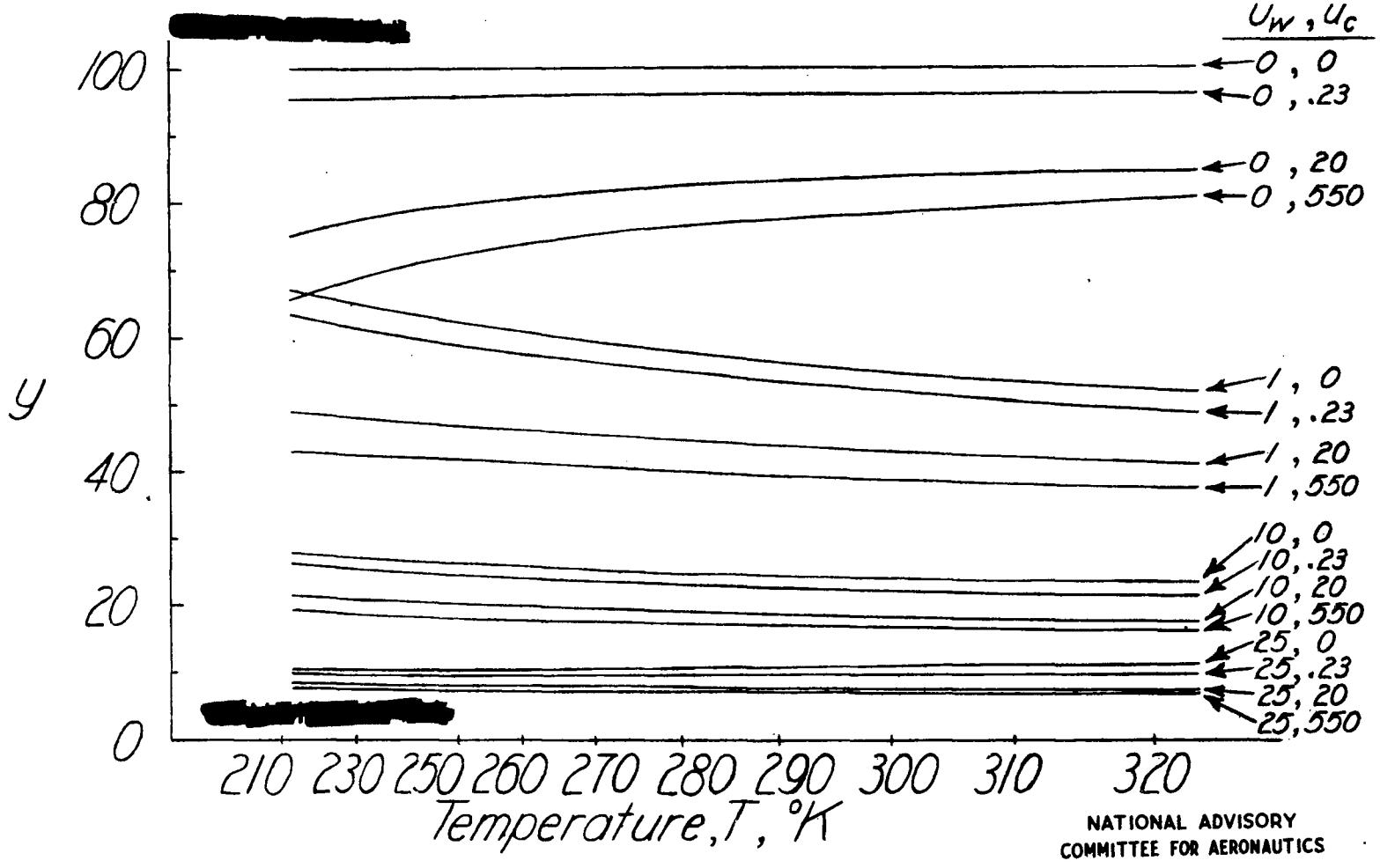

Figure 12.-Variation of y with absolute temperature for 16 combinations of water-vapor content u_w and of carbon-dioxide content u_c. (See equations (30) and (31).)

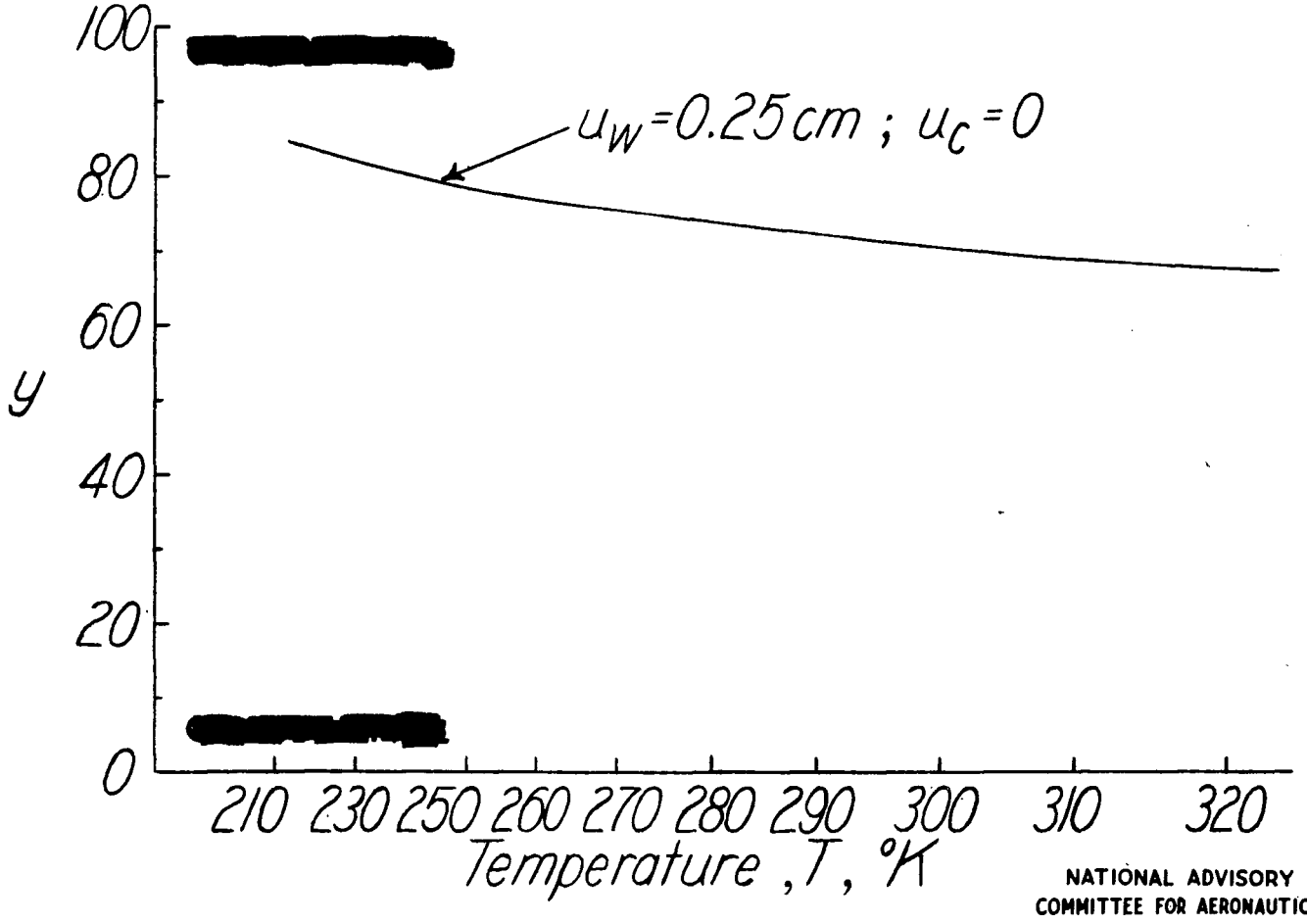

Figure 13.-Variation of y with absolute temperature for the combination of water-vapor content u_w and carbon-dioxide content u_c showing maximum variation of y with T.

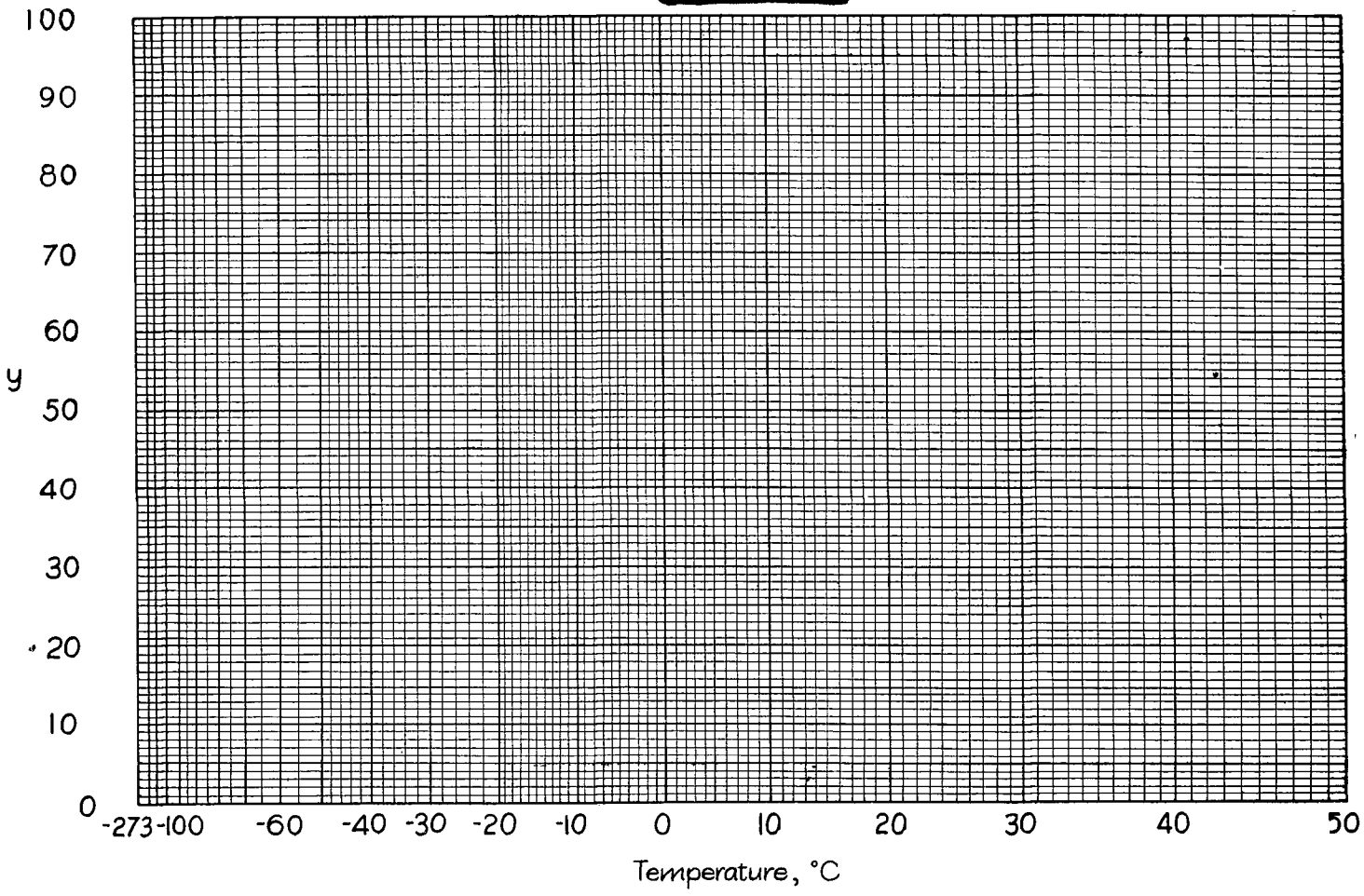

Figure 14.- Radiation chart applicable to the cloud indicator. Areas represent the exchange of radiation at the receiver of the cloud indicator. (For an incident beam of half-angle Θ, the entire ruled area represents $6560\pi \sin^2\Theta$ microwatts per cm^2 of aperture area.)

NATIONAL ADVISORY COMMITTEE FOR AERONAUTICS

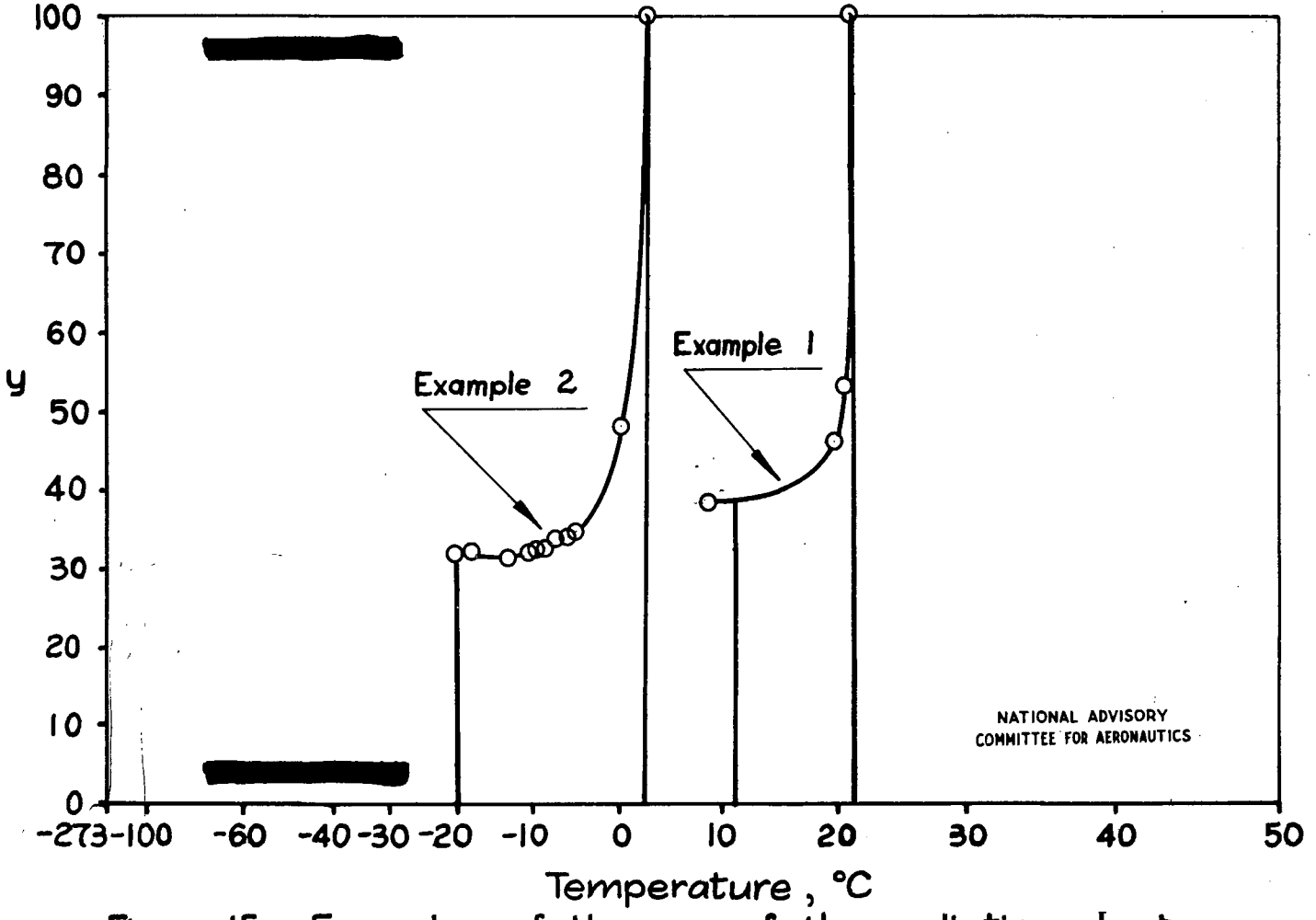

Figure 15.– Examples of the use of the radiation chart (fig. 14) and the radiation tables (tables II to VI) in determining the exchange of radiation between a cloud and the cloud indicator. (See appendix D.)

ATI- 8195

TITLE: An Infrared Cloud Indicator - I - Analysis of Infrared Radiation Exchange with Tables and Charl for Calibration of the Cloud Indicator

AUTHOR(S) : Warfield, Calvin N.; Kenimer, Robert L.

ORIG. AGENCY : Langley Memorial Lab., Langley Field, Va.

PUBLISHED BY : National Advisory Commiltee for Aeronautics, Washington, D. C.

DIVISION: (None)

SERIES AGENCY NO: (None)

PUBLISHING NO: ACR-L5104

DATE	U.S. CLASS	COUNTRY	LANGUAGE	PAGES	ILLUSTRATIONS
Nov '45	Unclass.	U. S.	English	76	tables, graphs, drawings

ABSTRACT:

Development of a device utilizing the thermal emission of infrared radiation that locates clouds at night and thereby enables the pilot to avoid them. A number of flight tests were made which conclusively demonstraled that the cloud indicator could detect the presence of clouds at night when they could not be seen with the unaided eye. Six parameters are used in an analysis of the net exchange of radiation between the receiver of the indicator and the cloud.

DISTRIBUTION: SPECIAL. Atl requests lor copies must be addressed to: Publishing Agency

DIVISION: Meteorology (30)

SECTION: Equipment and Instruments (9)

ATI SHEET NO.:

SUBJECT HEADINGS: Instruments, Meterorological (52201)
Instruments. Flight (52101)
Humidity indicators (49733)
Infrared radiallon (51912.8)

Central Air Documents Office
Wright-Patterson Air Force Base, Dayton, Ohio

AIR TECH INDEX

15